



HAL
open science

Formation and preservation of vertebrate tracks in semi-liquid sediments: Insights from tidal flats and laboratory experiments

Sonia Campos-Soto, Bernadette Tessier, Dominique Mouazé, M. Isabel Benito, I. Emma Quijada, Pablo Suarez-Gonzalez

► To cite this version:

Sonia Campos-Soto, Bernadette Tessier, Dominique Mouazé, M. Isabel Benito, I. Emma Quijada, et al.. Formation and preservation of vertebrate tracks in semi-liquid sediments: Insights from tidal flats and laboratory experiments. *Sedimentology*, 2024, 10.1111/sed.13224 . hal-04676866

HAL Id: hal-04676866





<https://hal.science/hal-04676866v1>

Submitted on 24 Aug 2024

HAL is a multi-disciplinary open access archive for the deposit and dissemination of scientific research documents, whether they are published or not. The documents may come from teaching and research institutions in France or abroad, or from public or private research centers.

L'archive ouverte pluridisciplinaire **HAL**, est destinée au dépôt et à la diffusion de documents scientifiques de niveau recherche, publiés ou non, émanant des établissements d'enseignement et de recherche français ou étrangers, des laboratoires publics ou privés.

Formation and preservation of vertebrate tracks in semi-liquid sediments: Insights from tidal flats and laboratory experiments

SONIA CAMPOS-SOTO* , BERNADETTE TESSIER†, DOMINIQUE MOUAZÉ† ,
M. ISABEL BENITO*·‡ , I. EMMA QUIJADA§ and PABLO SUAREZ-GONZALEZ* 
*Departamento de Geodinámica, Estratigrafía y Paleontología, Facultad de Ciencias Geológicas,
Universidad Complutense de Madrid, Madrid 28040, Spain (E-mail: sonia.campos.soto@ucm.es)
†Normandie Université, UNICAEN, UNIROUEN, CNRS, M2C, Caen 14000, France
‡Instituto de Geociencias IGEO (CSIC, UCM), Madrid 28040, Spain
§Departamento de Geología, Universidad de Oviedo, Oviedo 33005, Spain

Associate Editor – Massimiliano Ghinassi

ABSTRACT

Despite the valuable palaeoecological and palaeoenvironmental information provided by vertebrate tracks, those made in semi-liquid sediments have been largely overlooked because they are assumed to be preserved as a mass of disrupted sediment and to have a low preservation potential. Nevertheless, understanding their mechanisms of formation, infilling and preservation is crucial since they could be more abundant in the fossil record than expected or be misinterpreted as other soft-sediment deformation structures. To solve these aspects, this study analyses consecutive cross-sections performed along a human track made by a shod foot in semi-liquid sediments in the upper intertidal flats of the Bay of Mont-Saint-Michel (north-west France) and monitored until its complete burial. These were compared with cross-sections of tracks made in a flume tank. Cross-sections reveal that the sediment structures associated with these tracks reflect the mechanism of their formation and infilling, and even the footstep dynamics. These structures comprise: (i) marginal rims that developed at both sides of tracks during foot penetration; (ii) upward deformation structures produced during foot withdrawal; (iii) a *syn-track infilling*, which almost entirely fills the tracks during the withdrawal, formed by sediment collapsed from the track walls or by liquefied sediment; (iv) a *post-track infilling* that fills the tracks completely during their subsequent flooding. This work demonstrates that these tracks have a high preservation potential in tidal settings, especially if they are made after the peak of a spring tide period, and undergo desiccation and consolidation during neap tides, which prevents their erosion and favours their burial by sediment. The identification of the above-mentioned structures in fossil counterparts provides useful palaeoenvironmental information, because they allow discriminating these tracks from those made in sediments with less water content and from other soft-sediment deformation structures (i.e. convolute bedding and balls-and pillows) with which they share strong resemblances.

Keywords Bay of Mont-Saint-Michel, deep track, overtrack, sediment consistency, track infill, undertrack.

INTRODUCTION

Vertebrate tracks comprise distinctive sedimentary structures that result from the complex interaction between the sediment and the track-maker (e.g. Falkingham, 2014). Their proper recognition in the fossil record is crucial since they provide essential keys for deciphering the palaeoecology and palaeoenvironments of ancient deposits, as well as the behaviour of the track-makers (e.g. Lockley, 1986; Brand & Tang, 1991; Marty, 2008; Alcalá *et al.*, 2014; Castanera *et al.*, 2014; Falkingham, 2014; Melchor, 2015; D'Orazi *et al.*, 2016; Campos-Soto *et al.*, 2017, 2019; Díaz-Martínez *et al.*, 2018). Track identification in the fossil record is commonly associated with the recognition of downward deformation structures that may display different morphological features, such as the outline of the foot and toes, the impressions of some anatomical details (i.e. claw or pad marks, among others) and even the marginal folds caused by the plastic deformation of the sediment around the foot (e.g. Loope, 1986; Allen, 1997; Milàn, 2006; Marty *et al.*, 2009; Avanzini *et al.*, 2012; Melchor, 2015). In fact, the recognition of the impressions of anatomical details, such as skin, in ancient vertebrate tracks allows discriminating the sediment that was in direct contact with the foot (that is, the true track) from the underlying deformed sediments (undertracks) and from the sediments infilling the track (overtracks), which are very useful features for performing palaeoichnological interpretations (e.g. Thulborn, 1990; Lockley, 1991; Gatesy, 2003; Marty *et al.*, 2009).

The morphological preservation of anatomical features (*sensu* Marchetti *et al.*, 2019), or the anatomical fidelity (*sensu* Gatesy & Falkingham, 2017), are mainly related to the water content of the sediment when the track is made: it is commonly better in sediments with moderate to low water content (e.g. Allen, 1997; Marty *et al.*, 2006, 2009; Milàn, 2006; Marty, 2008; Milàn & Bromley, 2008); on the contrary, in sediments with high water content it is much poorer, since liquefaction occurs as the foot penetrates into the sediment, inducing the collapse of the track walls, which are processes that obliterate track morphology, as reported in modern sediments (e.g. Allen, 1997; Milàn, 2006; Marty *et al.*, 2009; Marchetti *et al.*, 2019) and in laboratory-controlled experiments (Milàn & Bromley, 2008; Jackson *et al.*, 2009, 2010). For these reasons, tracks made in semi-liquid

sediments have been overlooked many times, because they are assumed to be simply preserved as a 'mass of disrupted sediment' and to have a low preservation potential (Allen, 1997).

Recent studies have demonstrated that misidentification of tracks made in semi-liquid sediments (also called penetrative tracks; Falkingham *et al.*, 2020; Gatesy & Falkingham, 2020; Lallensack *et al.*, 2022) has led to interpreting them incorrectly as produced by thin-toed animals or plantigrade locomotion (Gatesy & Falkingham, 2020; Lallensack *et al.*, 2022). Nevertheless, even though these tracks are not suitable for the identification of the possible track-maker, some studies have claimed their usefulness for reconstructing the foot motion within the sediment (Avanzini, 1998; Gatesy *et al.*, 1999; Gatesy, 2003; Falkingham *et al.*, 2020; Turner *et al.*, 2020). A few laboratory-controlled experiments have reproduced some of the deformation structures they could make in homogeneous or artificial sediment and have evaluated their potential to produce undertracks (Milàn & Bromley, 2006, 2008; Jackson *et al.*, 2009, 2010). However, many vertebrate tracks of the fossil record are preserved in fine-grained heterogeneous laminated sediments, i.e. alternating silty and clayey beds, especially those deposited in tidal settings (e.g. Allen, 1997; Marty *et al.*, 2009; Alcalá *et al.*, 2014; Castanera *et al.*, 2014; D'Orazi *et al.*, 2016; Campos-Soto *et al.*, 2017). It is therefore necessary to reproduce new experiments in heterogeneous sediments, in which vertebrate tracks could also be recorded. The analysis of this type of track in such conditions will allow to better understand the variability of sedimentary structures that they could produce during their formation and to establish criteria for their proper identification, since they may be more abundant in the fossil record than expected. For example, these tracks may have been misinterpreted as other soft-sediment deformation structures (SSDS) that are commonly associated with deformation and liquefaction of water saturated sediments under the action of a variety of triggering events, such as earthquakes, tidal bores or overload (Loope, 1986; Melchor, 2015; Díaz-Martínez *et al.*, 2018; Carvalho *et al.*, 2021). Furthermore, considering that tracks made in semi-liquid sediments are prone to erosion by currents, it is still necessary to understand the post-formational processes that could favour their infilling, burial and preservation, since, to the authors' knowledge, there are no studies that evaluate their preservation potential in the fossil record.

The present work aims to understand the mechanisms of formation, infilling and preservation of vertebrate tracks made in semi-liquid sediments and to provide criteria for their recognition in the fossil record, but not to provide keys allowing the recognition of the specific track-maker and the analysis of its locomotion. It rests on an experimental approach developed mainly in the field and complemented in the laboratory. For field experiments, human shod foot tracks were made in semi-liquid sediments in the upper intertidal flats of the estuary of the Bay of Mont Saint Michel (BMSM, north-west France; Fig. 1). The BMSM offers well-developed heterogeneous laminated tidal facies made up of fine-grained sediments (clayey silt to very fine sand), favourable for the formation and preservation of a large variety of sedimentary structures and traces (Bajard, 1966; Tessier, 1993, 2002; Lanier & Tessier, 1998; Tessier *et al.*, 2021), including abundant vertebrate tracks (Campos-Soto *et al.*, 2022a, 2022b). These sediments are very similar to some track-bearing deposits of the fossil record (Quijada *et al.*, 2013, 2016; Campos-Soto, 2020), which makes them an ideal analogue for carrying out these experiments. For laboratory experiments, tracks were produced in a flume tank, in sediments collected from the BMSM, in which tidal couplets were recreated. The analysis of both field and laboratory tracks has allowed: (i) to analyse the mechanisms of creation of the sedimentary structures produced during the formation of vertebrate tracks in semi-liquid tidal sediments and those produced during their infilling; (ii) to understand the hydrodynamic conditions and associated sedimentary processes that favour their preservation in the sedimentary record; (iii) to identify the position of the true track, undertracks and overtracks in this type of track, which will be useful when analysing their fossil counterparts; (iv) to establish the criteria to recognize vertebrate tracks made in semi-liquid sediments in the fossil record, to discriminate them from tracks made in sediments with less water content and, more importantly, to distinguish them from other SSDS. The fact that the experiments performed in this work are made by shod foot, prevents from exploring additional palaeobiological and palaeoecological implications, but will serve for comparison with other ancient deposits including shod human tracks (e.g. Duveau *et al.*, 2021; Kyparissi-Apostolika & Manolis, 2021; Ledoux *et al.*, 2021; Helm *et al.*, 2023).

STUDY SITE

The BMSM is located in the north-western coast of France, along the south-eastern margin of the English Channel (Fig. 1A and B). It is a wide (500 km²) and shallow (<20 m) wedge-shaped bay that extends between the Cotentin Peninsula (Normandy) and the Brittany Coast (Fig. 1A and B). Its substrate corresponds to the Precambrian rocks of the Armorican Massif (L'Homer *et al.*, 1999). Its sedimentary infilling mainly occurred during the Holocene transgression, i.e. since about 8000 years BP (Larsonneur *et al.*, 1989; Billeaud, 2007; Tessier *et al.*, 2010). Sedimentary dynamics in the bay are nowadays strongly controlled by tidal currents (Larsonneur *et al.*, 1989). The tidal range reaches up to 15.3 m during the highest spring tides (Caline, 1982; Larsonneur *et al.*, 1989; Tessier, 1993). The tidal regime is semi-diurnal with a very small diurnal inequality (Tessier *et al.*, 1995).

Three different morphosedimentary settings are distinguished in the bay (Fig. 1B; L'Homer *et al.*, 1999; Caline *et al.*, 2002; Tessier *et al.*, 2006): (i) a sandy littoral, to the north-east, formed by sandy beaches and aeolian dunes; (ii) a tide-dominated estuary, to the east, formed by the junction of three rivers (Sée, Sélune and Couesnon), which traverse intertidal and supratidal flats and are characterized by a negligible fluvial discharge (Caline, 1982; Larsonneur *et al.*, 1989); and (iii) a non-estuarine embayment, to the west, that comprises extensive intertidal to supratidal flats.

Specifically, the study area is situated at the transition between the outer and the inner part of the estuary and, more precisely, in the upper intertidal flats developed at the Pointe du Grouin du Sud locality, along the bank of a small tidal channel (Figs 1B to 1D and 2A). The estuary is subject to a progressive reduction of the tidal current velocity (Larsonneur *et al.*, 1989; L'Homer *et al.*, 1999; L'Homer & Caline, 2002). This produces a gradual decrease of the sediment grain size from pebbles at the outer subtidal areas, to muddy-silty sediments at the supratidal flats of the inner estuary (L'Homer *et al.*, 2002; Bonnot-Courtois, 2012). At the Pointe du Grouin du Sud, the sediments of the upper intertidal flats, on which the tracks were made, consist of very fine-grained silty-sands to clayey-silts that include more than 50% of carbonate of bioclastic origin (fragments of molluscs, foraminifera, ostracods, coccoliths, echinoderm spines and bryozoans), as well as quartz and mica grains and

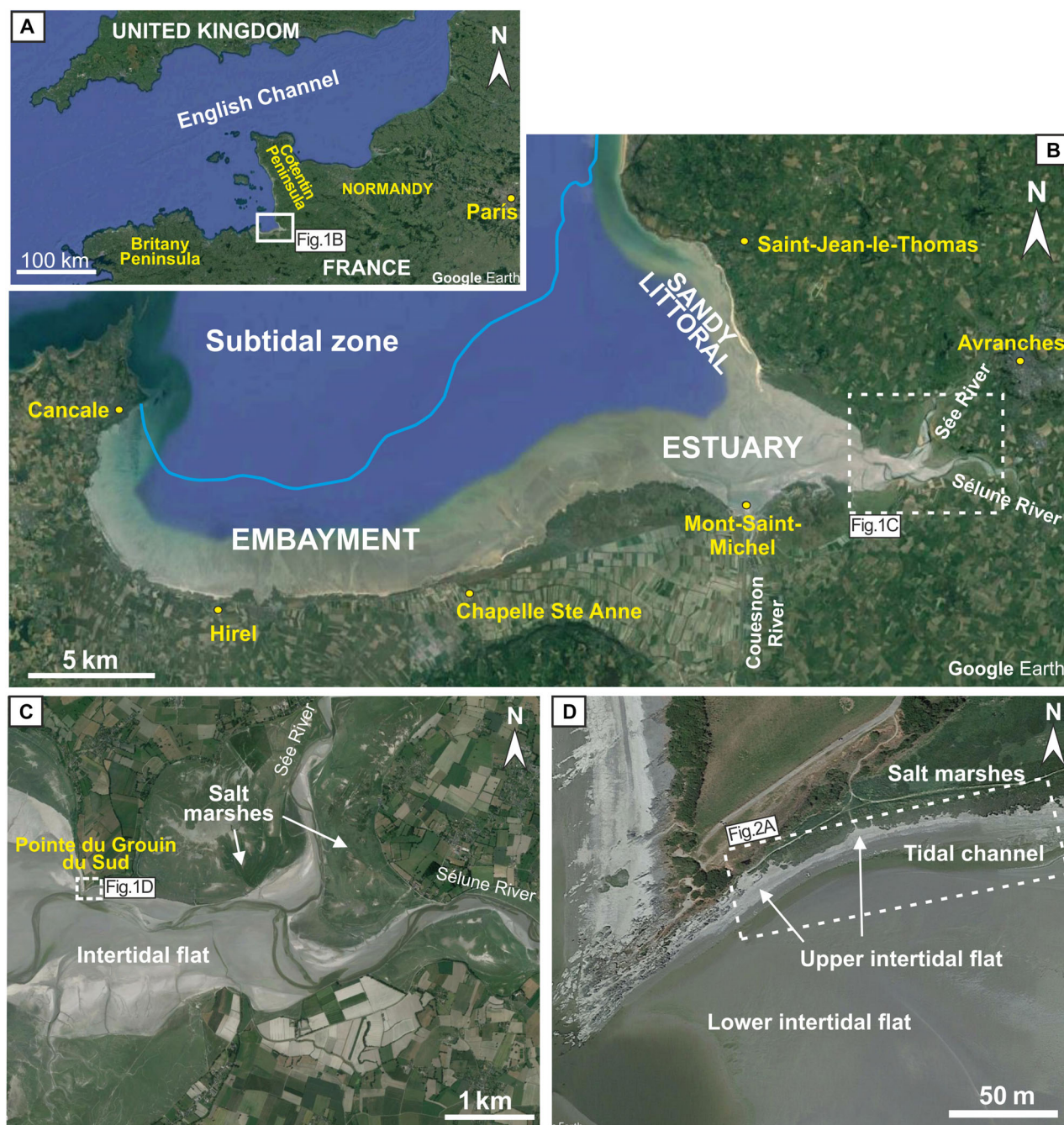


Fig. 1. Satellite images of the study area. (A) Location of the Bay of Mont-Saint-Michel (BMSM) in the south-eastern margin of the English Channel, in north-west France. (B) The three morphosedimentary environments recognized in the BMSM: the sandy littoral, the estuary and the embayment. (C) Location of the study area, Pointe du Grouin du Sud, within the inner estuary. (D) South-eastern part of Pointe du Grouin du Sud, showing the upper intertidal flats where the human tracks were made.

heavy minerals (Boucart & Charlier, 1959; Larsonneur *et al.*, 1989; Tessier, 1993, 2002; L'Homer *et al.*, 1999; Billeaud, 2007). The size, composition and morphometry of the particles confer to

this sediment specific properties that allow the formation and preservation of a great variety of sedimentary structures. In cross-section, this sediment displays a laminated appearance, formed

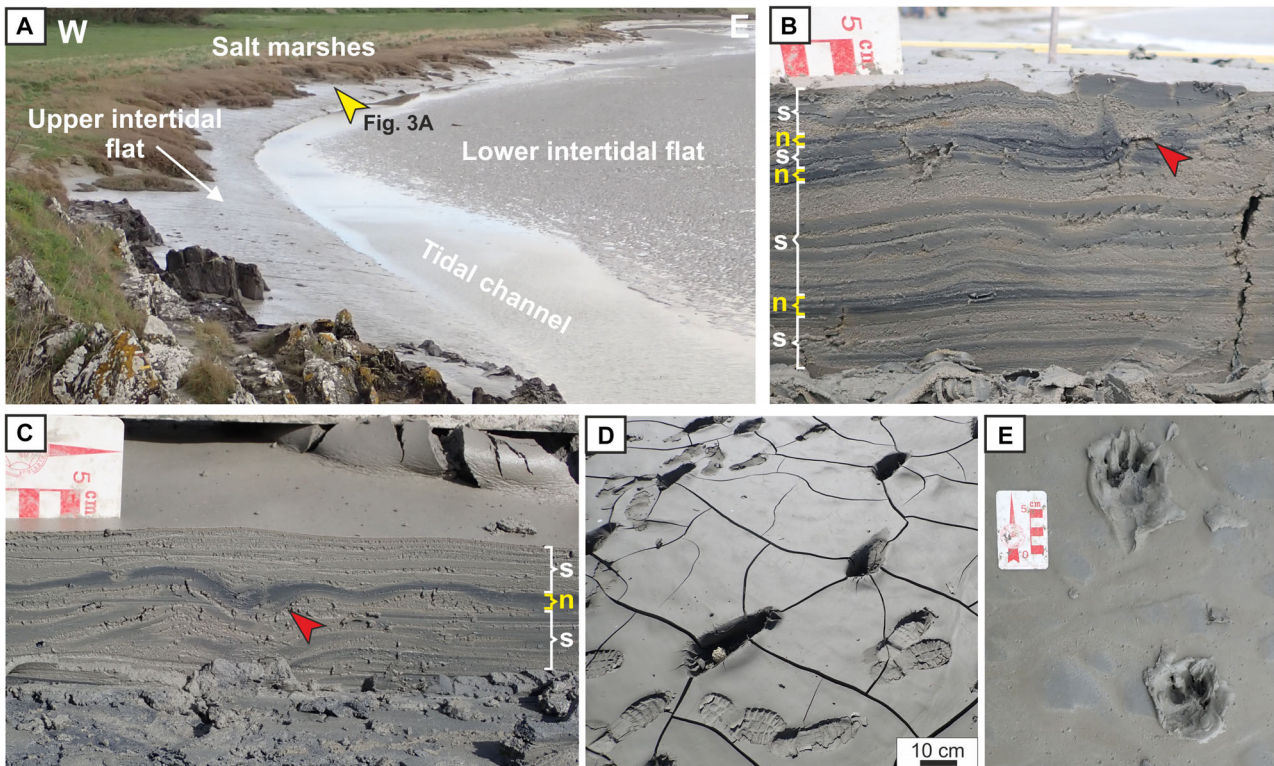


Fig. 2. Field photographs of the study area located at Pointe du Grouin du Sud. (A) Panoramic view of the upper intertidal flats, where the human tracks were made. Note how they are delimited by salt marshes, to the west, and by a tidal channel and lower intertidal flat areas, to the east. (B) and (C) Upper intertidal sediments made up of an alternation of sandy and muddy sediments organized in neap (n) and spring (s) cycles (yellow and white arrows, respectively). Note the occurrence of vertebrate tracks (red arrows) within these sediments. (D) Upper intertidal sediments displaying human trackways and large desiccation cracks. (E) Trackway made by a dog in the upper intertidal sediments.

by millimetre to centimetre-thick sandy-silt and clayey-silt couplets, giving rise to flaser, wavy, lenticular and planar-bedding (Fig. 2B and C; Tessier, 1993, 2002; Billeaud *et al.*, 2007). Moreover, these couplets progressively thicken and thin out upward, displaying tidal rhythmites (Fig. 2B and C; Tessier, 1993, 2002; Tessier *et al.*, 1995). Each couplet represents the sedimentary record of one tide. Deposition of these couplets only occurs during spring tides, because this is the only moment of the fortnightly (neap–spring–neap) tidal cycle when the upper intertidal flats get covered by tides (Tessier, 1993). During neap tides, the upper tidal flat is subject to long periods of emersion, leading to the development of abundant desiccation cracks (Fig. 2D; Tessier, 1993, 2002; Billeaud *et al.*, 2007). In addition, the occurrence of invertebrate bioturbation in these sediments is very scarce due to the high rate of sedimentation and strong fluctuations

of salinity and temperature that occur in this area of the estuary (Tessier *et al.*, 1995; Tessier, 2002).

Properties of these upper intertidal sediments not only enhance the preservation of tidal sedimentary structures, but also of vertebrate tracks (Fig. 2D and E). These tracks deform the underlying layers and are afterwards covered by sediments during the following tides, leading to their preservation (Fig. 2B and C; Campos-Soto *et al.*, 2022a, 2022b).

METHODS

Two experiments have been carried out: (i) a field experiment, in which the processes of formation of human tracks (feet in rubber water boots) and their post-formation evolution under natural conditions have been analysed (Figs 3 to 6); (ii) a laboratory experiment, in which the

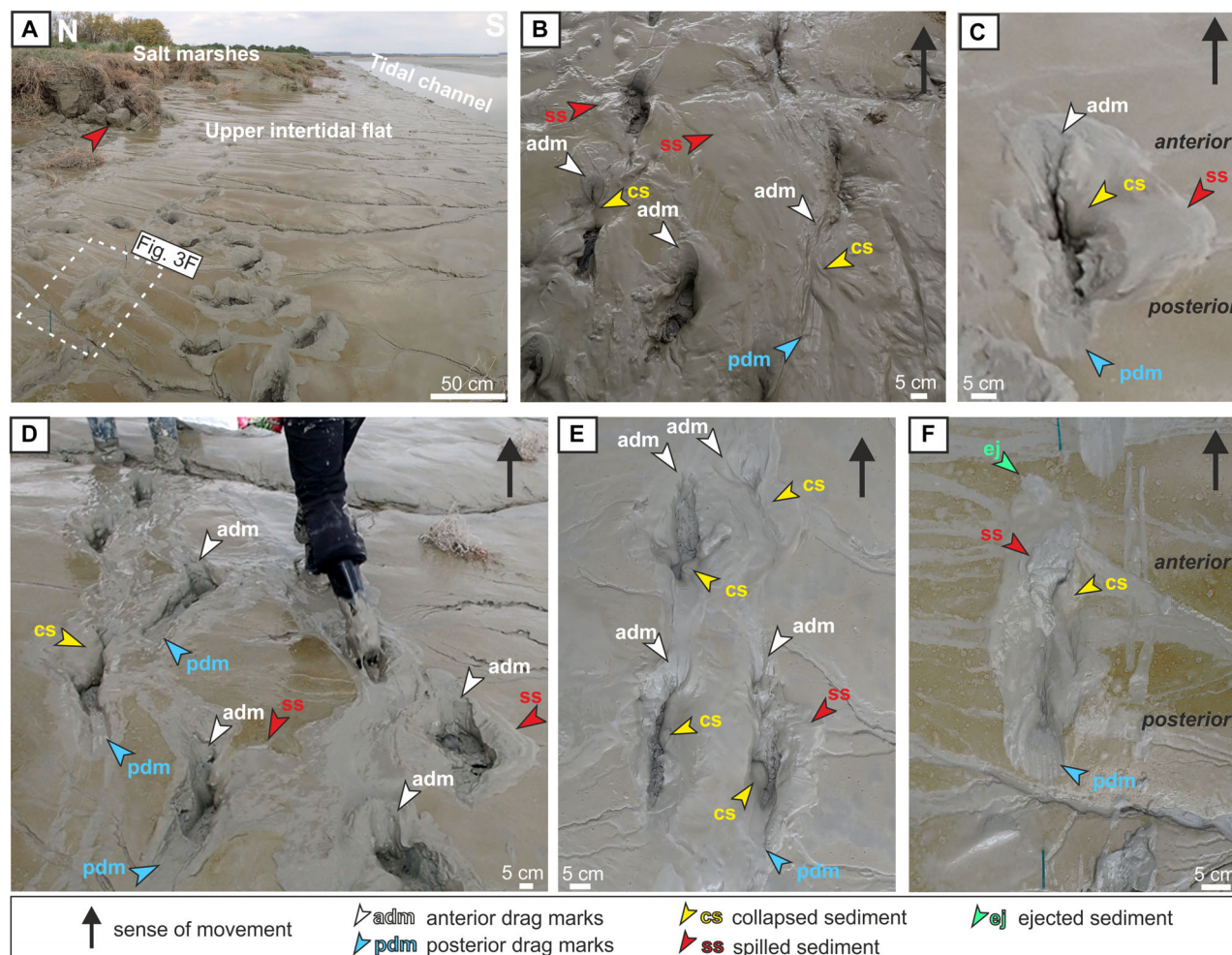


Fig. 3. (A) General view of the upper intertidal flats at Pointe du Grouin du Sud, where the human tracks were made in a semi-liquid sediment. Note the occurrence of some large muddy blocks that come from the erosion of the salt marsh deposits (red arrow). The white rectangle marks the position of the track shown in Fig. 3F, which was the track selected for studying its post-sedimentary evolution through time (see details in Fig. 4). (B) to (F) Field photographs of human tracks and trackways made in semi-liquid sediments. Tracks display very poorly defined shapes as they are filled by sediment collapsed from their walls (yellow arrows). Some of the tracks are filled partially or almost completely by the collapsed sediment. Tracks that are completely filled just remain as very small depressions over the surface – see tracks located in the lower right part of (B), in the upper right part of (E) and in (F). The sediment collapse is not symmetrical, as evidenced by the location of the largest accumulations of collapsed sediment in different areas within each track. Additionally, tracks display drag marks at their posterior and anterior parts (blue and white arrows, respectively), which record the movement of the feet when entering and going out of the sediment, respectively. Tracks may also display marginal folds made up of deformed or spilled sediment (red arrows). Note in (B) and (D) how the spilled sediment is larger in one of the sides of the tracks, as it depends on the area where the feet exerted more pressure when walking (red arrows). Some ejected sediment could also be deposited several centimetres ahead of tracks during the withdrawal of the feet – green arrow in (F).

mechanisms of track formation made by a plastic rod were analysed in a flume (Figs 7 and 8). In both experiments, the term ‘*track*’ refers to the impression left by the human shod feet or the plastic rod when they penetrated into the sediment (Marty *et al.*, 2016). In order to clearly

separate processes that occur due to the formation of tracks and the sedimentological ones that occur subsequently, this study will use the term ‘*syn-track infilling*’ for that formed by sediment that collapses from the track walls and/or by liquefied sediment, and ‘*post-track infilling*’ for

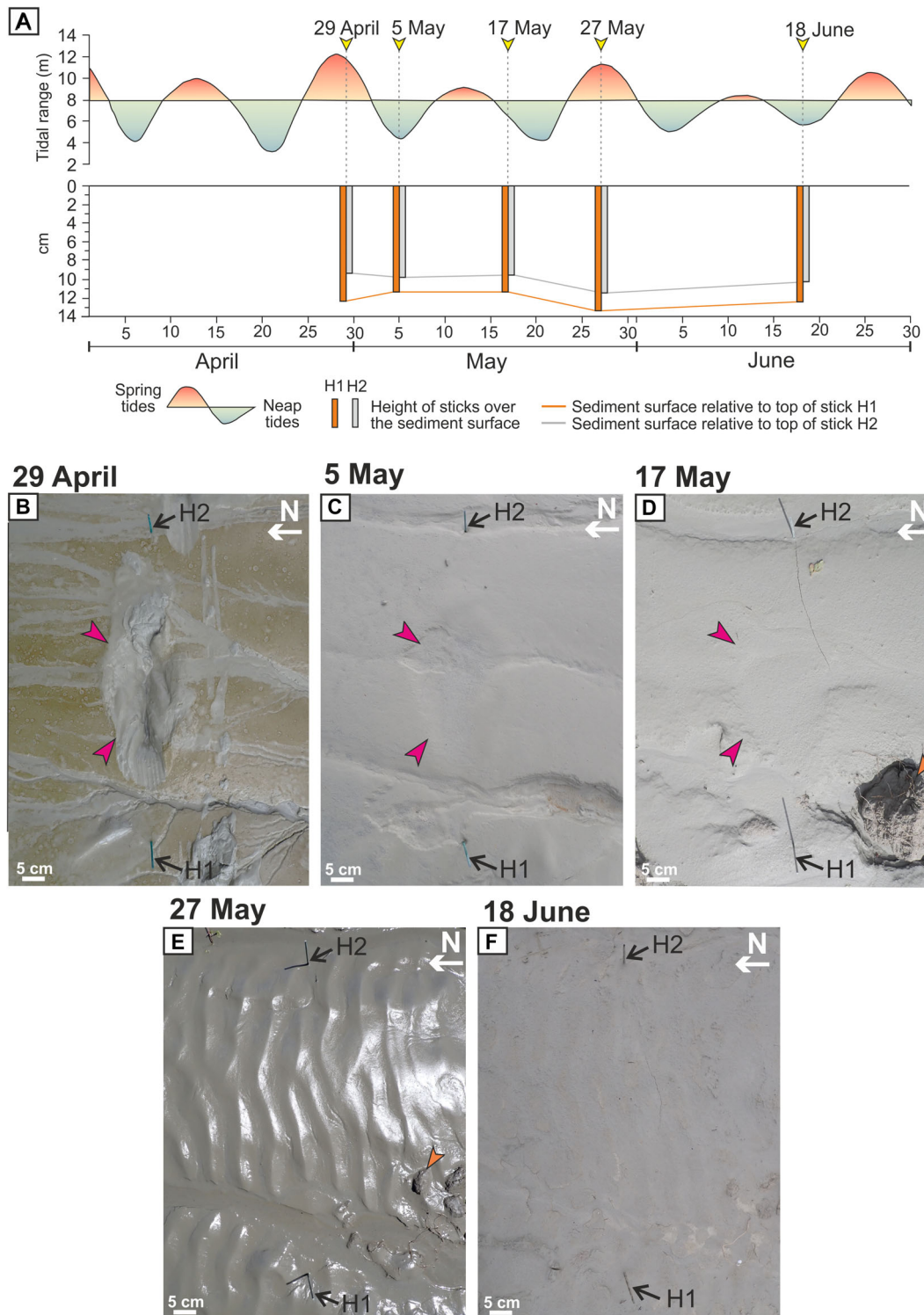


Fig. 4. Post-sedimentary evolution of a human track made on 29 April 2021 and monitored until 18 June 2021. (A) Graph showing the evolution of the tidal range from April to June 2021 (data obtained from the French Naval Hydrographic and Oceanographic Service – SHOM) and the measured heights of the two sticks (H1 and H2) located behind and in front of the track, respectively (see Fig. 4B to F). The yellow arrows indicate the days when the track was visited. (B) to (F) Photographs of the human track monitored for seven weeks until it was completely covered by sediment. Pink arrows mark the position of the track. Orange arrows point to some mud pebbles that came from the erosion of the salt marshes (see examples in Fig. 3A).

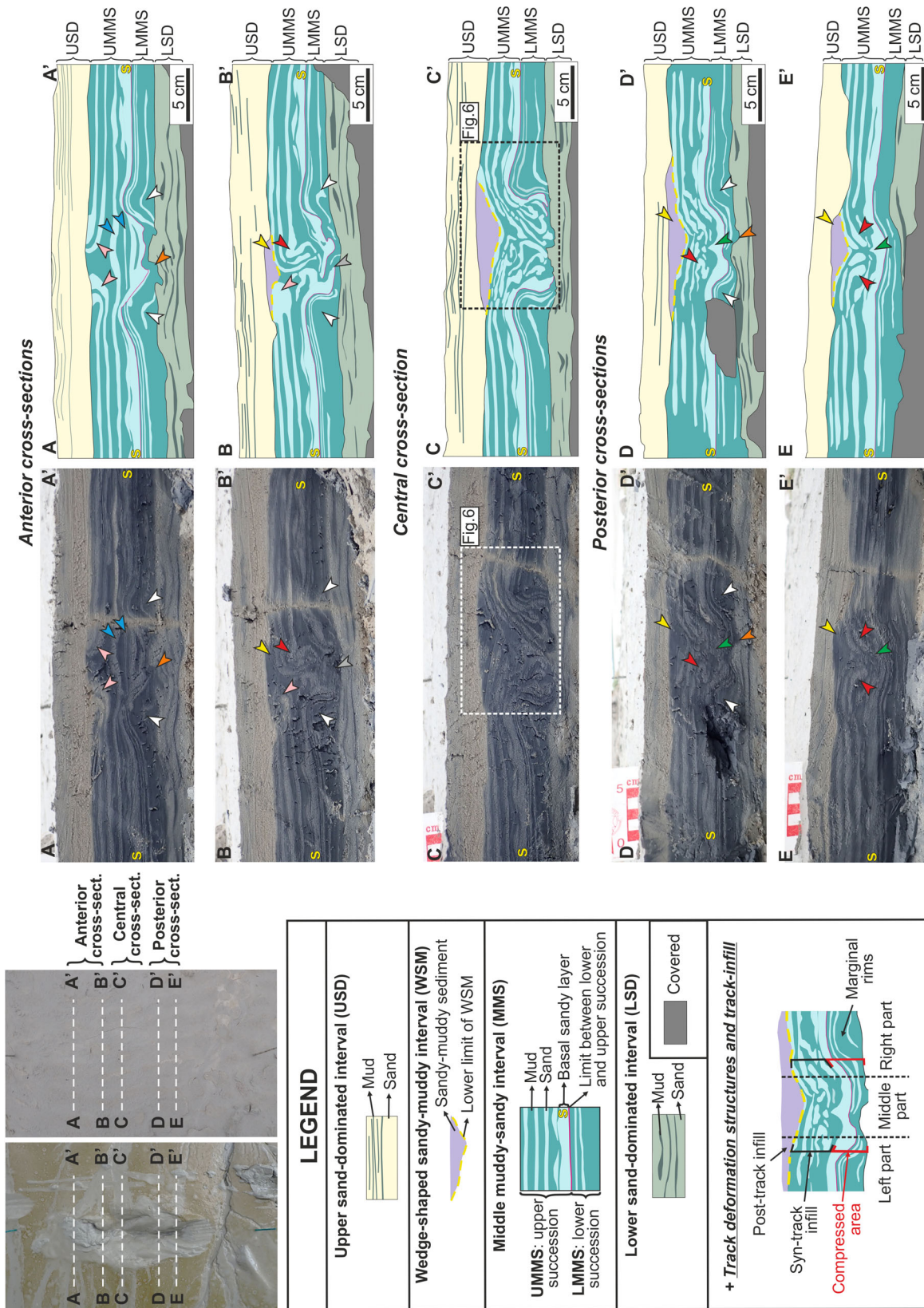


Fig. 5. Cross-sections and line drawings of the human track-bearing sediments. Track-bearing sediments comprise, from base to top: a *lower sand-dominated interval* (LSD), which is just slightly deformed in the area located below the track (orange arrow); a *middle muddy-sandy interval* (MMS), which includes the deformation produced by the track and the *syn-track infilling* (red arrow), and comprises a lower muddier succession (LMMS) and an upper sandy-muddy succession (UMMS); a *wedge-shaped sandy-muddy interval* (WSM), which includes the *post-track infilling* – or overtrack – (yellow arrow); and an *upper sand-dominated interval* (USD), which was deposited after the complete infilling of the track. White arrows point to the marginal folds formed during the penetration of the foot at both sides of the track. Green arrows point to sediments that were deformed upward due to the suction produced during the withdrawal of the heel. Grey arrow points to the sediments that have been broken and displaced in the compressed area of the anterior cross-section B–B'. Red arrows mark the occurrence of folded layers of sediment, which correspond to the *syn-track* sediment that collapsed inside the track. Blue arrows point to some horizontal layers interpreted to be compressed by the foot and rebounded during its withdrawal as a consequence of the suction effect. Pink arrows indicate the position of the sediment layers that were deformed upward during the withdrawal of the anterior part of the foot, during which the sediment is pushed ahead of the track.

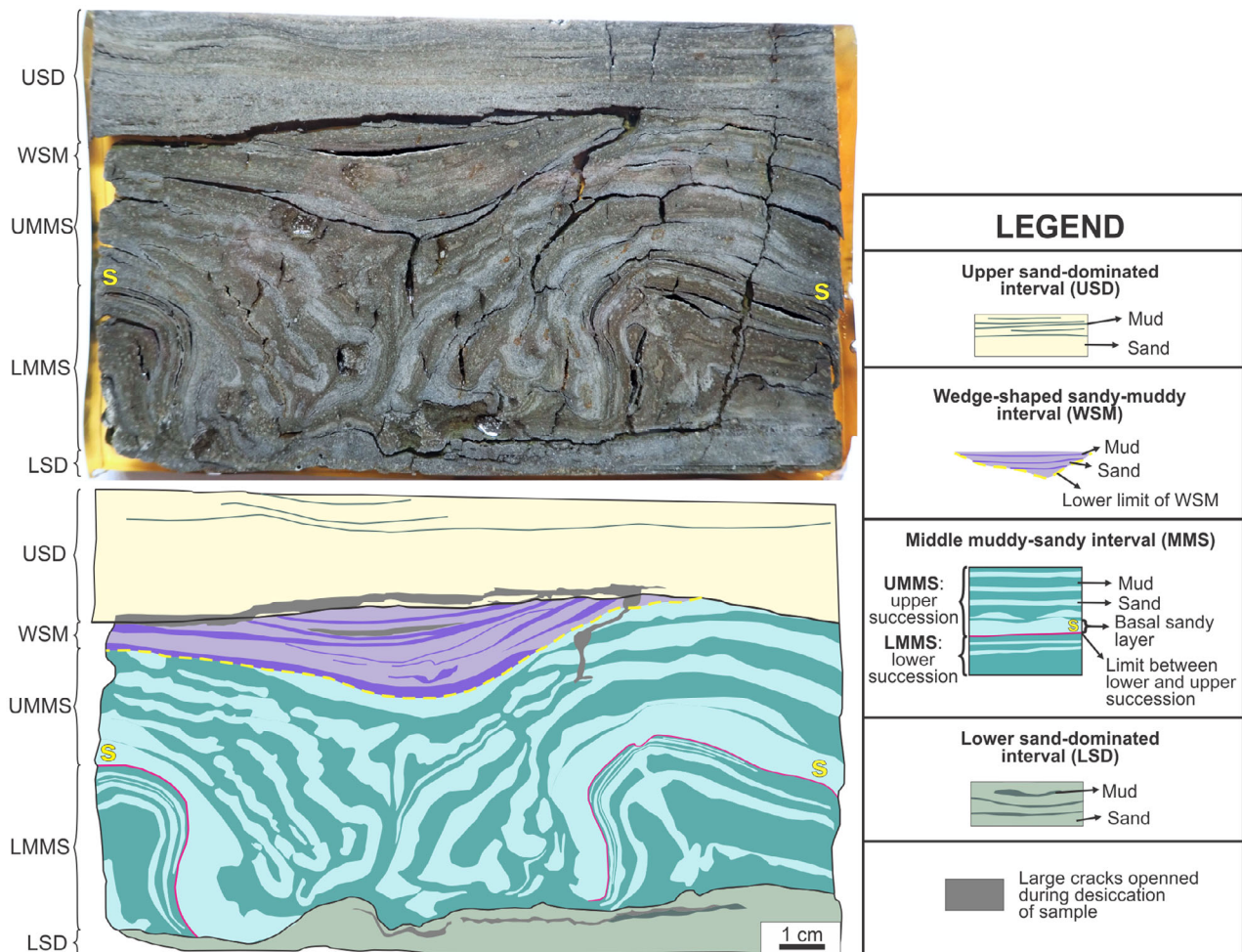


Fig. 6. Photograph (above) and line drawing (below) of sediments collected in the central cross-section of the human track, showing the *syn-track* and *post-track* sediments infilling the track (see location of area sampled in the cross-section C–C' in Fig. 5). Note that the *post-track* infilling is internally formed by a laminated sandy-muddy sediment.

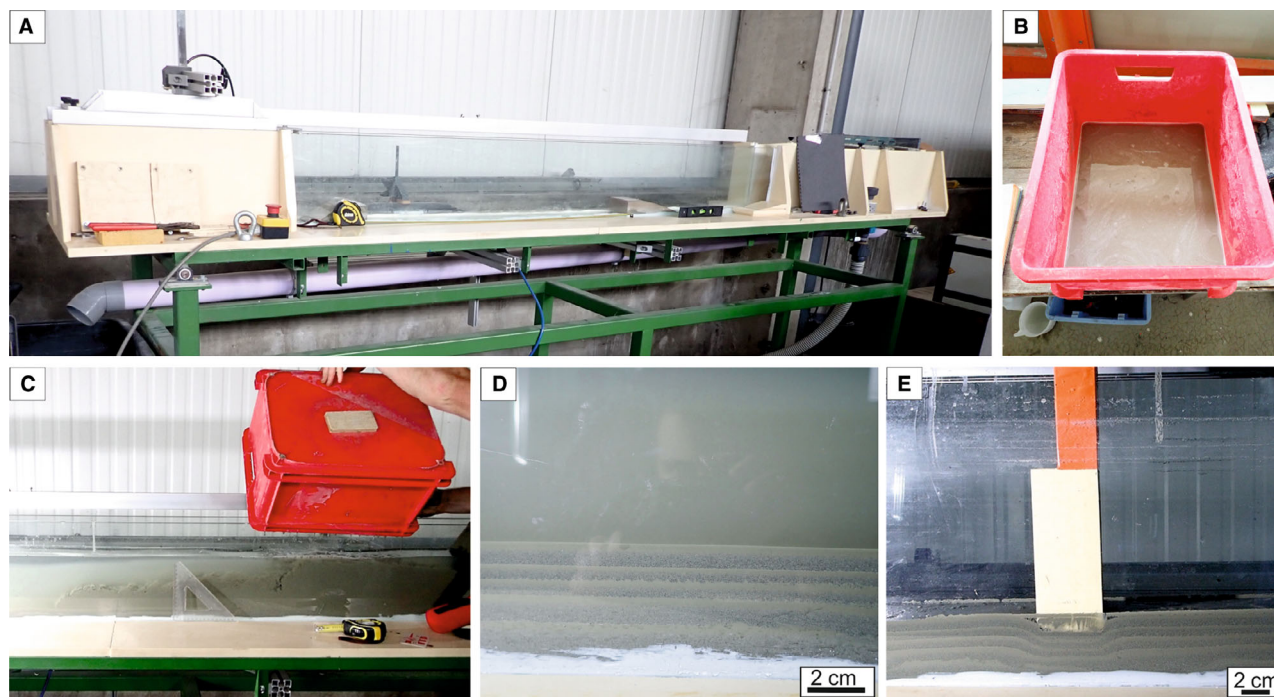


Fig. 7. (A) Erodimeter flume of the Laboratoire Morphodynamique Continentale et Côtière of the Université de Caen Normandie–CNRS, where the laboratory tracks were made. (B) and (C) Photographs of the protocol followed for recreating the characteristic tidal lamination in the sediments sampled from the BMSM. (B) Mixture of the same quantities of the sediment sampled from the BMSM and water. (C) Pouring of the mixture of sediment and water into the flume, which was previously filled with a water column of 15.5 cm. (D) Sandy-mud couplets created by the decantation of the sediment poured into the flume. (E) Tracks were made in the laminated sediment by using a rectangular section (2.8 × 5.0 cm) plastic rod.

that filling the tracks during subsequent flooding. The morphological features of tracks and sediment consistency (i.e. degree of firmness) are described in this work following the nomenclature proposed by Allen (1997).

Field experiment

Human tracks were made in semi-liquid silty-clayey sediments (mean grain-size around 50 µm) deposited in the upper intertidal flat of Pointe du Grouin du Sud during several field trips carried out during 2021 (Figs 3 and 4). Water content of such semi-liquid sediments freshly deposited at high tide on upper flats reaches up to 90 to 100% with respect to dry sediment weight. Tracks were made by a 55 kg person using rubber boots 24 cm long and up to 10 cm wide, having a flexible sole (see Video S1 of the supplementary material). Tracks were also photographed and described in order to analyse their morphology and the features produced

during the track-making process, and to follow their post-sedimentary evolution afterwards.

From all of the tracks made in semi-liquid sediments, some of them were selected to analyse their evolution through time (Fig. 4A to 4F). Their location was georeferenced with a GPS and marked with two wooden sticks that were inserted deep into the sediment, and several centimetres behind and in front of the track, following its longitudinal axis (Fig. 4). The length and maximum width of the tracks were also measured; no data of their maximum depth could be taken as the sediment of the track walls collapsed just immediately after the foot was withdrawn (see Video S1 of the supplementary material). Then it was only possible to monitor one of these tracks during the whole field experiment, because the wooden sticks that identified the others had disappeared.

The track was monitored on four occasions over the next seven weeks, which allowed to observe and to photograph its evolution through

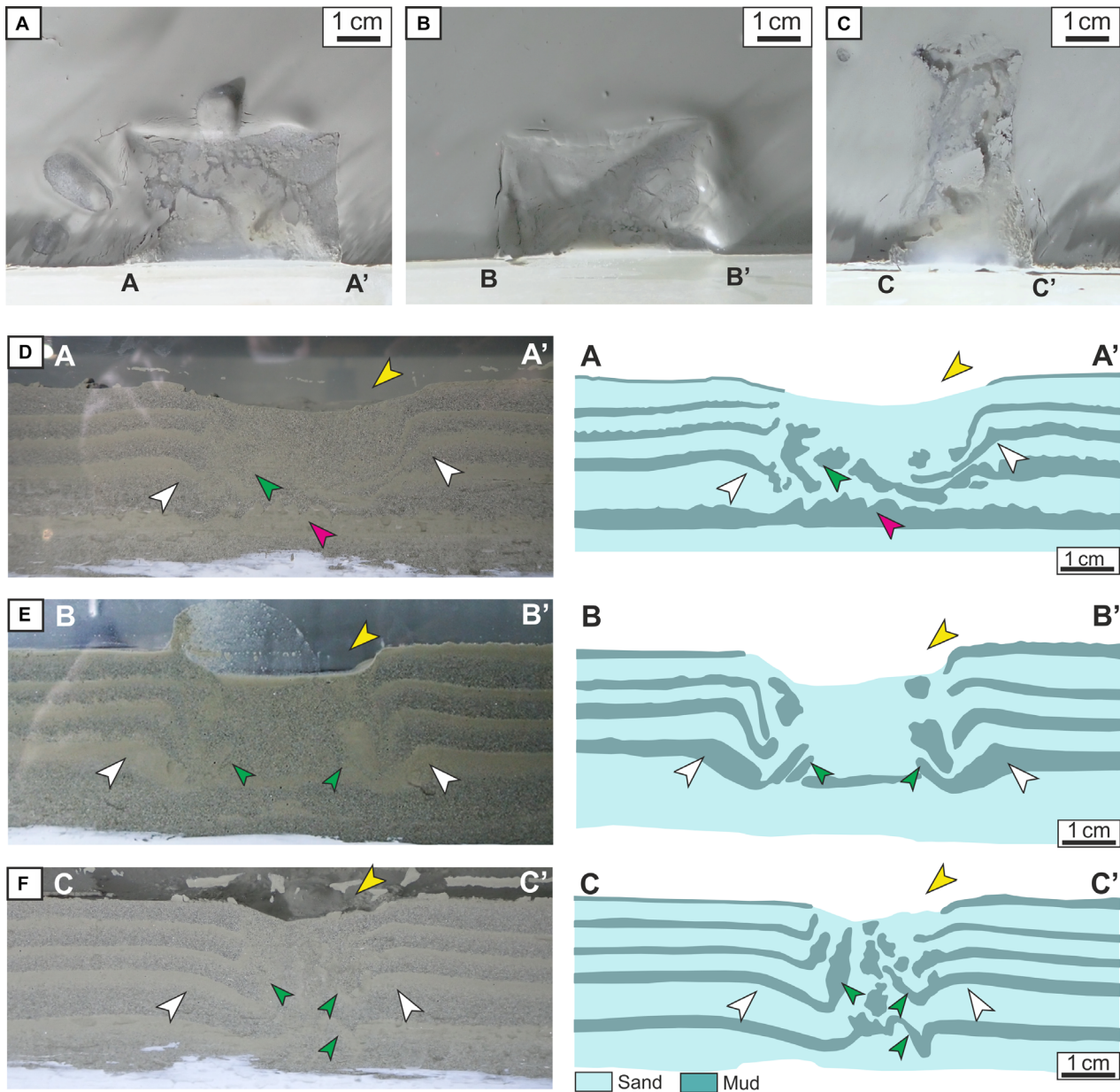


Fig. 8. Tracks made in the experimental flume in plan view (A) to (C) and in cross-section view (D) to (F). Note that the tracks shown in (A), (B), (D) and (E) were made by placing the long side of the plastic rod parallel to the glass of the flume, while the track shown in (C) and (F) was made by placing its short side parallel to the glass. (A) to (C) Plan view of tracks displaying poorly defined shapes and remaining as small depressions in the surface after being filled by liquefied sediment. (D) to (F) Cross-sections of tracks displaying marginal folds (white arrows) and *syn-track* infillings made up of liquefied sediment. Green arrows point to the deformed layers placed below the liquefied sediment. Pink arrow marks the load and flume structures produced in the lowermost muddy layer. Yellow arrow points to the small depression located above the track.

time and its progressive covering by sediment (Fig. 4). The height of the wood sticks outside of the sediment was measured at each visit in order to identify episodes of erosion and/or

sedimentation (Fig. 4A). Values of tidal range were analysed in order to evaluate the periods when the track was covered by tides. These values were obtained from the tide gauge located

in Saint-Malo, which are provided by the French Naval Hydrographic and Oceanographic Service (SHOM, <https://maree.info/52>).

Once the track was completely covered by sediment, a series of cross-sections were made into the sediment, at the emplacement of the track and perpendicular to its longitudinal axis (Fig. 5). These cross-sections allowed analysing the deformation structures produced during the track-making process and the track infilling. A plastic box (17 × 10 × 4 cm) was used to obtain a representative sample from the sediment deformed by the track and its infilling (Fig. 6). This sample was later completely dried out in the laboratory, embedded with epoxy resin and polished for performing subsequent laboratory analysis and photographs.

The structures observed in the cross-sections were then compared with those of other vertebrate tracks preserved within upper intertidal sediments of the inner estuary of the BMSM, in order to assess whether the structures that characterize experimental tracks are easy to recognize in the sedimentary record, and whether they are observed frequently, which would demonstrate that tracks made in semi-liquid sediments may be easily preserved. The structures were also compared with other soft-sediment deformation structures in order to establish criteria for distinction.

Laboratory experiment

The experiment was carried out in the indoor erodimeter flume of the Laboratoire Morphodynamique Continentale et Côtière of the Université de Caen Normandie-CNRS (Fig. 7A). The flume, 10 cm wide, is formed by transparent glass walls 2 m long and 20 cm high. It is connected to a recirculating water system, fed by a pump, which enables to fill and empty it with water. The sediment introduced into the flume was collected from the upper intertidal flats of the inner estuary of the BMSM and, thus, is similar to the sediment of the field experiment site but slightly sandier. During its sampling, the typical tidal bedding of the sediment was destroyed. Thus, in order to reconstruct a couplet succession into the flume, the sediments sampled in the field were deposited through decantation. For this purpose, a mixture of 2 kg of sediment and 2 kg of water was poured into the flume, which was previously filled with water, in order to obtain a first 'sand–mud' couplet, approximately 2 cm thick and 1 m long

(Fig. 7B and C). For the following couplets, a mixture of 1 kg of sediment and 1 kg of water was poured each time, which allowed creating individual sand–mud couplets 1 cm thick and 1 m long (Fig. 7D). A time interval of approximately 3 h passed between the deposit of each couplet to allow consolidation of the recently deposited sediment and to prevent its erosion during the following pouring of sediment. Once a couplet succession of significant thickness was obtained (representing a total of five couplets) the flume was slowly emptied of water. After 4 h, when the sediment was still highly saturated in water, three tracks were made with a plastic rod with rectangular section (2.8 × 5.0 cm; Fig. 7E). The rod was manually pushed down into the sediment, following a vertical trajectory, until it reached the lowermost 2 cm thick 'sand–mud' couplet, and was later removed upward vertically. Tracks were made very close to the frontal glass wall of the flume, which allowed observing in cross-section the structures produced in the sediment during the track-making and withdrawal processes (Fig. 7E). The videos showing the formation of two tracks are provided in supplementary material (see Video S2 and S3).

RESULTS

Field experiment

Making human tracks in semi-liquid upper intertidal sediments

The analysis of human tracks made in semi-liquid sediment deposited in the upper intertidal flats at Pointe du Grouin du Sud, has allowed to study the different processes that occurred during the track-making process under the specific conditions of the present field experiments, i.e. with respect to the sediment properties and behaviour of the track-maker (Fig. 3). The part of the foot that first entered into contact with the sediment was the heel, because it is a specific aspect of the human way of walking (Alexander, 2004). When the heel touched the sediment, it slipped few centimetres on the surface, leaving a drag mark that could be observed in the posterior part of tracks (blue arrows in Fig. 3B to F; see Video S1). Immediately after this slipping, the whole foot sank into the semi-liquid sediment, penetrating several centimetres until it eventually reached a firmer sediment layer. During its penetration, the semi-

liquid sediment surrounding the foot could get deformed or even get spilled out of the track (red arrows in Fig. 3B to E; see Video S1).

As the forward motion of the foot continued, the metatarsal applied more pressure to the underlying sediment in order to impulse the movement. This pressure could induce that this part of the foot penetrated few centimetres deeper into the sediment, allowing the heel to rise. As the heel withdrew, the sediment of the track walls started to collapse within the track (yellow arrow in Fig. 3E; see Video S1). When the front part of the foot was going out of the sediment, it pushed the sediment located above and in front of it, spilling it out towards the anterior part of tracks (red arrows in Fig. 3F). Small amounts of sediment could be also ejected and deposited several centimetres ahead of the tracks (green arrow in Fig. 3F). During this withdrawal movement, the foot also produced some drag marks in the sediment located in the anterior part of tracks (white arrows in Fig. 3B to E). Immediately after the toes were completely out, the sediment located in the walls at the anterior part of the tracks also collapsed inside of them (yellow arrows in Fig. 3B to F; see Video S1). Depending on how the withdrawal movement of the foot was performed, the amount of collapsed sediment could be different from one side of the wall to the other and/or from the posterior to the anterior parts of tracks (Fig. 3B, D and E). Furthermore, depending on the amount of sediment that collapsed inside the tracks, they could be filled partially or almost completely. In the latter, tracks remained as very small depressions over the surface (Fig. 3B, E and F; see Video S1).

Monitoring the post-sedimentary evolution of a human track through time

The monitored track was made on 29 April 2021, one day after the peak of an equinoctial spring tide period, which was characterized by a maximum tidal range of 12.4 m (Fig. 4A). It was made in muddy water-saturated sediment colonized at the surface by a brownish diatom biofilm (Fig. 3F). The track showed a poorly defined shape and remained as a small depression over the surface, as it was almost completely filled by the sediment that collapsed from the walls (Figs 3F and 4B). At the posterior and central parts of the track, the collapsed sediment filled the track symmetrically, while the anterior part was only filled by the sediment

that had collapsed from the right wall (see yellow arrow in Fig. 3F). At the anterior part, there was also some sediment that had been spilled slightly leftward, but mainly forward of the track (red arrow in Fig. 3F). Some ejected sediment was deposited several centimetres ahead of the track (green arrow in Fig. 3F). In addition, drag marks were observed at the posterior part of the track (blue arrow in Fig. 3F).

The selected track was visited, on 5 May, during the following neap tide period (Fig. 4A and C). At that moment the track was almost completely refilled by muddy-silty sediment. Only a vestige of its shape and a very shallow depression could be noticed. The track was visited again on 17 May, during the next neap tide period and after a small spring tide period (maximum tidal range of 9.3 m; Fig. 4A and D). The shape of the track was barely noticeable (Fig. 4D). A muddy block, 10 cm wide, which came from the erosion of the nearby salt marshes, was deposited behind the track (orange arrow, Fig. 4D). On 27 May the track was visited during the peak of the following spring tide period (maximum tidal range of 11.4 m; Fig. 4A and E). The monitored surface was covered by two-dimensional sandy ripples that were draped by a millimetre thick layer of silty mud. Small muddy blocks, up to 3 cm wide, were locally observed on top of the sandy ripples. The last visit occurred on 18 June, during a neap tide period (Fig. 4A and F). Since the previous visit a neap and a small spring (maximum tidal range of 8.5 m; Fig. 4A) tide periods had taken place. The only visible features of the sediment surface were the faint crests of some sandy ripples.

The height measurements of sticks H1 and H2, located behind and in front the track, respectively (Fig. 4B), allowed to recognize erosive or sedimentation events that occurred at the monitored surface. During the first two visits (5 and 17 May), minor variations (1 cm maximum) were detected on the height of the sticks (Fig. 4A), in relation with local and slight erosion or accretion processes occurring along small drainage rills (Fig. 4B to D). On 27 May, an erosion of 2.0 cm and 1.5 cm on sticks H1 and H2, respectively (Fig. 4A), was recorded. This erosional phase occurred prior to the deposition of the sandy ripples observed during that visit (Fig. 4E). Finally, an episode of slight accretion (1 cm) was recorded on 18 June (Fig. 4A).

Sedimentary analysis of the track-bearing sediments

Four main sedimentary intervals were recognized in the cross-sections of the track-bearing sediments (Figs 5 and 6), which correspond, from base to top, to:

1 A *lower sand-dominated interval* (LSD), which is slightly deformed by the track at its uppermost part. It comprises up to 3.3 cm thick fine-grained sand alternating with millimetre thick discontinuous muddy layers, forming flaser bedding (Fig. 5). These sediments were deposited during spring tides because this is the only period of the fortnightly tidal cycle when the tidal range is sufficiently high for the tides to flood the upper tidal flats (Tessier, 1993, 2002).

2 A *middle muddy–sandy interval* (MMS), which includes the deformation structures produced by the track and the sediment that collapsed inside it during foot withdrawal (Figs 5 and 6; see detailed description of the track in the following section). These sediments display a relatively flat contact with the underlying LSD, except in the area located just below the track, where the contact is irregular (see details in the following section). The MMS comprises up to 8.3 cm thick alternating muddy and fine-grained sandy layers. Sandy layers may be flat or display ripples. The sediments of this interval are grouped into two thinning-upward successions: (i) a lower succession (LMMS), which is muddy dominated and displays lenticular bedding; and (ii) an upper succession (UMMS), which starts at the base with a 1 cm thick rippled sandy layer (level ‘S’ in Fig. 5), followed upward by alternating sandy and muddy layers, displaying wavy bedding. The lower succession is interpreted as the result of deposition during a spring–neap cycle, as has been similarly interpreted in upper intertidal sediments of the bay (Tessier, 1993, 2002). The thickest layers located at the base of the succession represent deposition during the peak of spring tides, whereas the thinning-upward layer represents the progressive decrease in tidal energy from spring to neap tides (Tessier, 1993, 2002). The upper succession is interpreted as formed during the spring tide period at the end of April, just immediately before 29 April, when the track was made (Fig. 4A). Sediments of both successions are involved in the deformation structures produced by the track.

3 A *wedge-shaped sandy–muddy interval* (WSM), which overlies the deformation structures and the collapsed sediment that filled the track during foot withdrawal (see purple interval in Figs 5 and 6). The WSM comprises a wedge-shaped layer up to 2.2 cm thick that shows a concave base and pinches out laterally (Figs 5 and 6). Internally, it is made up of laminated sandy–muddy sediment (Fig. 6). According to observations during monitoring, these sediments are interpreted as the infilling of the small depression left after the collapse of sediment by the tides that flooded the upper intertidal flats immediately after the track-making (see track on 5 May in Fig. 4C) and during the tides of the following small spring tide period (see track on 17 May in Fig. 4D).

4 An *upper sand-dominated interval* (USD), which overlies the sediments of the WSM and MMS with an erosive contact (Figs 5 and 6) and includes the sediments deposited after the complete infilling of the track. Sediments of the USD are up to 4.5 cm thick and comprise millimetre to centimetre-thick fine-grained sandy layers, which are flat or display ripples, and are draped by millimetre-thick muddy layers. This interval was probably deposited during the spring tides that took place at the end of May, as indicated by the presence of sandy ripples at that moment (see track on 27 May in Fig. 4E). In addition, the stick height evolution confirms that a significant deposition took place between the peak of the spring tide period at the end of May and the neap tide period in mid-June (Fig. 4A). The tidal range of the spring tide period around 10 June was too small to induce deposition; thus, the USD deposition can be associated with the spring tide period of the end of May. The erosive surface at the base of the USD indicates that erosional processes occurred before deposition. This erosive episode, denoted by the stick height evolution between mid-May and the end of May (Fig. 4A), can be associated with the highest velocity tidal currents that occurred around the peak of the spring tide period of the end of May.

Track deformation structures and track infilling

The deformations produced by the human track mainly involve the sediments of MMS and, to a much lesser degree, the uppermost part of the LSD (orange arrows in Fig. 5). The sand-dominated LSD interval is firmer, preventing the

downward propagation of the deformation. Similar intervals were described as ‘*decollement*’ or ‘*detachment*’ levels by Allen (1997) and Marty (2008) in some Holocene and Kimmeridgian mammal and dinosaur track-bearing deposits, respectively.

The human track deforms all the layers of the LMMS and UMMS. However, the degree of deformation of the sediments differs from the LMMS to the UMMS and from the posterior to the anterior cross-sections of the track (Fig. 5). In these cross-sections the sediments of the LMMS and the lowermost sandy layer (S) of the UMMS are thinner in the middle part of the track, i.e. in the area where they were compressed by the foot, and get thicker in the marginal folds that are formed at both sides of the track (see white arrows in sections A–A’, B–B’, D–D’ and E–E’ in Fig. 5). In the central cross-section, the sediments of the LMMS and the sandy layer (S) have completely vanished in the middle part of the track and they are displaced laterally, giving rise to large marginal folds (see section C–C’ in Fig. 5; Fig. 6). This indicates that the metatarsal of the foot penetrated deeper into the sediments with respect to the heel and the toes. This process was noticed during the track-making process, because the foot had to exert a greater pressure below the metatarsal to impulse its forward movement (see *Making human tracks in semi-liquid upper intertidal sediments*). The distance measured between the marginal folds is also larger in the central cross-section (where it reaches up to 7.4 cm) with respect to the anterior and posterior ones (Fig. 5), because the metatarsal is wider in comparison to the heel and toes. Additional differences in the degree of deformation produced by the track are recorded in the anterior and posterior cross-sections. In the anterior cross-section B–B’, the sediments of the LMMS and the sandy layer (S) of the UMMS are broken and displaced at the left part of the compressed area (see grey arrow in section B–B’ of Fig. 5) in addition to showing a different degree of deformation at the right part. Taking into account that the track was made with the left foot, these structures might indicate that the internal side of the foot applied a different pressure than the external part. Similar examples have been reported in some vertebrate tracks preserved in Jurassic tidal and aeolian deposits by Marty (2008) and Graversen *et al.* (2007), who described the occurrence of fractures in the sediment compressed by the foot and interpreted

them as the result of the shift in the weight distribution of the foot during the track-making process. In the posterior cross-sections D–D’ and E–E’, the basal sandy layer (S) of the UMMS is deformed slightly upward in the compressed area (see green arrow in sections D–D’ and E–E’ of Fig. 5). This deformation could have resulted from the suction effect that is produced during the withdrawal of the heel. Equivalent structures have been observed in some tracks made in water-saturated sandy sediments in laboratory-controlled experiments (see *Laboratory experiment* section), which were caused by the adhesion of sediment to the plastic indenter during its withdrawal (Jackson *et al.*, 2009, 2010).

Sediments overlying the sandy layer (S) of the UMMS are deformed downward, filling the space located above the compressed sediments between the marginal folds. Sandy layers of this deformed UMMS are characterized by highly distorted outlines that pinch out laterally and by folds that are inclined towards the inner part of the track. Such features indicate that these sediments correspond to the semi-liquid sediment that collapsed from the track walls during and immediately after the withdrawal of the foot. They are named here the *syn-track infilling*.

The structures displayed within the *syn-track infilling* sediments clearly reflect the processes observed during the removal of the foot from the semi-liquid sediment (see section *Making human tracks in semi-liquid upper intertidal sediments*). For example, in the central and posterior cross-sections, the sediment from both sides of the track is almost symmetrically deformed downward towards the compressed area (see sections C–C’ to E–E’ in Fig. 5; Fig. 6), indicating that the sediment collapsed simultaneously from both walls, as observed in the plan view of the track in Fig. 3F. The anterior cross-sections show some differences compared to the central and posterior ones. In the anterior cross-section B–B’, all the layers of the UMMS located at the right part of the track are deformed towards its inner part, displaying a large fold located above the compressed sediments (see red arrow in section B–B’ in Fig. 5). This large fold was produced as a result of the collapsing of sediment from the right wall of the track after the withdrawal of the foot, as could be observed in the plan view of the track (see yellow arrow in Fig. 3F). In the anterior cross-section A–A’, the uppermost sediments of the UMMS do not show lateral continuity and are deformed upward in the middle part of the track (see pink

arrows in section A–A' in Fig. 5). Similarly, the anterior cross-section B–B' also shows how the uppermost layers located at the left part of the track are deformed upward (see pink arrow in section B–B' of Fig. 5). These features result from the upward deformation of the sediment during the withdrawal of the anterior part of the foot, when the sediment was pushed outside of the track (see red arrow in Fig. 3F). In addition, in the anterior cross-section A–A', in the compressed area, there are some horizontal layers located above the basal sandy layer (S) of the UMMS and below the uppermost layers that are slightly deformed upward (see blue arrows in section A–A' in Fig. 5). These horizontal layers are interpreted to be compressed by the toes and later rebounded as a consequence of the suction effect that was produced during the withdrawal.

The cross-sections highlight the significant difference in the deformation style between the LMMS and the UMMS, which can be directly related to the difference of sediment consistency with depth. The sediments of the LMMS are interpreted to have been deposited during the spring tide period around 12 April 2021 and were subaerially exposed during the following neap tide period. Thus, they were necessarily more compacted and have lower water content than those of the UMMS, which were deposited at the end of April, when the track was made. Moreover, sediments of the LMMS have a greater proportion of mud than those of the UMMS (Fig. 5), which makes them more cohesive. Consequently, sediments of the LMMS were plastically deformed when they were compressed by the foot, getting thinner in the middle part of the track and thicker in the marginal folds. Sediments of the UMMS overlying the basal sandy layer (S), very freshly deposited when the track was made, collapsed inside the track during and after foot withdrawal, giving rise to highly distorted outlines and folds inclined towards the compressed area. It is important to remark that the thick sandy layer (S) located at the base of the UMMS is deformed conformably with the sediments of the LMMS (more consistent), not as the rest of the UMMS (more fluid). The greater consistency of this sandy layer S and the LMMS has controlled the depth of penetration of the foot, as the sandy layer S corresponds to the level until which the track penetrates in most cross-sections, being cut only in the central one, which is the area where the metatarsals applied the greatest pressure (Figs 5 and 6).

Finally, cross-sections show, above the UMMS, a small wedge-shaped layer of sandy–muddy sediment (see purple interval in Figs 5 and 6), which corresponds to the WSM. This sediment has been deposited during the subsequent flooding of the track by tides (see Fig. 4B), and it is named here the *post-track infilling*.

Laboratory experiments

Laboratory experiments have allowed the authors to directly observe the behaviour of semi-liquid sediment when pressured by a plastic rod with rectangular section in plan (Fig. 8A to C) and cross-section (Fig. 8D to F), and to compare it with the semi-liquid sediment behaviour observed in the field experiment. Cross-sections allowed analysing the structures produced along the longitudinal (Fig. 8D and E) and transverse sides (Fig. 8F) of the plastic rod.

Tracks were made following a simple vertical trajectory, both during the penetration and the withdrawal of the rod (see videos of tracks shown in Fig. 8A and B in Videos S2 and S3, respectively). When the plastic rod penetrated into the sediment, it produced the downward deformation of sediment layers, giving rise to the marginal folds at both sides of the tracks (see white arrows in Fig. 8D to F; see Videos S2 and S3). The rod penetrated until it reached the thick lowermost sandy–muddy couplet, producing deformation or breaking of the lowermost muddy layer, or even producing load and flame structures in it (see pink arrow in Fig. 8). As the rod descended, it produced the compression and liquefaction of sediment. This liquefied sediment almost completely filled the track when the rod was withdrawn (Fig. 8D and E; see Videos S2 and S3), producing the *syn-track infilling*. During the withdrawal, some of the compressed layers of sediment that were not liquefied, got deformed upward due to the suction effect (see green arrows in Fig. 8D to F; see Videos S2 and S3). This was especially noticed in the cross-section of the transverse side of the plastic rod (green arrows in Fig. 8F). These upward deformations are similar to the '*subsurface withdrawal rims*' made by experimentally reproduced emu bird tracks in water saturated sandy sediments (Jackson *et al.*, 2010), due to sediment uplift during foot withdrawal. The distance measured between the marginal folds after the removal of the rod ranges from 1.8 cm in the transverse cross-section (Fig. 8F) to 3.6 cm in the longitudinal cross-sections (Fig. 8D and E).

Once the tracks were filled by *syn-track* liquefied sediments during the withdrawal of the rod, they remained as small depressions in the surface (Fig. 8A to C, and yellow arrows in Fig. 8D to F; see Videos S2 and S3), which correspond to the only space available for being filled by *post-track sediments*.

DISCUSSION

Dynamics of vertebrate track formation in semi-liquid sediments

Both field and laboratory experiments have revealed that tracks made in semi-liquid sediments get almost completely filled during the track-making process (*syn-track infilling*). The human tracks were filled by the semi-liquid sediment that collapsed from their walls during and after foot withdrawal. Those made in the laboratory were filled when the plastic rod withdrew by liquefied sediment produced by the rod penetration. Similar mechanisms of track infilling by collapsed or liquefied semi-liquid sediment have been previously reported in plan view of human tracks made in modern tidal flats (Allen, 1997; Marty *et al.*, 2009), of Triassic theropod tracks made in lake deposits (Gatesy *et al.*, 1999) and of Middle Jurassic tridactyl tracks (Manning, 2004); additionally, in cross-sections of Lower Jurassic tidal deposits (Avanzini, 1998), and even in plan views and cross-sections of experimentally reproduced tracks made in homogeneous sandy sediments (Jackson *et al.*, 2009, 2010), in concrete (Milàn & Bromley, 2006, 2008) or in organic-rich muddy soil and glacio-fluvial sand (Milàn, 2006). In these examples, it is documented how the morphology of the track is highly distorted after being filled by collapsed or liquefied sediment. This has been similarly observed in the plan views of the studied tracks made in the field and the laboratory, which display very poorly defined morphologies (Figs 4B and 8A to C, respectively).

The fact that the human tracks were filled by collapsed sediment and that the laboratory tracks were filled by liquefied sediment results from their difference in composition: the sediment used in the flume tank being sandier (Fig. 8D to F) than the muddier sediment of the field. This has been similarly documented in other experimentally reproduced tracks made in water saturated conditions, which were filled by liquefied sediments when made in sandy

sediments (Jackson *et al.*, 2009, 2010), or by collapsed sediment when made in concrete (Milàn & Bromley, 2006, 2008). Furthermore, diatom biofilms present at the sediment surface in the field (for example, Fig. 3F) could have contributed to enhance cohesivity (Stal, 2012; Gerbersdorf & Wieprecht, 2015) and, thus, to reduce liquefaction.

The track-making process, in both human and laboratory tracks, led to the formation of marginal folds at both sides of the tracks during the penetration of the foot or plastic rod (white arrows in Figs 5 and 8D to F). Such folds are very common in other modern (e.g. Allen, 1997; Marty *et al.*, 2009) and ancient vertebrate tracks (e.g. Avanzini, 1998; Marty, 2008; Cariou *et al.*, 2014; Milàn *et al.*, 2021) made in sediments with moderate to high water content. Moreover, both human and laboratory tracks display upward deformed sediment layers due to the suction effect during withdrawal (green arrows in Figs 5 and 8D to F). Similar deformations have been reported in other experimental tracks in water saturated sediments due to the adhesion or uplift of sediment during the withdrawal (Milàn & Bromley, 2006; Jackson *et al.*, 2009, 2010). Jackson *et al.* (2009, 2010) also reported the occurrence of displacement bulbs below the *syn-track infilling*, which consist of small pockets of undeformed sediments that were pressed downward during the track-making process. These displacement bulbs have been considered by these authors as characteristic features of tracks made in semi-liquid sediment. They have not been identified in the studied human and laboratory tracks due to the fact that the experiments of Jackson *et al.* (2009, 2010) were made in homogeneous sandy sediments with no variation of consistency with depth, which allowed a deeper transmission of the deformation. In contrast, the studied human tracks were made in heterogeneous muddy and sandy sediments, whose consistency increases with depth, and overlie the firmer sandy sediments, which impeded the further penetration of tracks and the downward transmission of deformation (see Fig. 5 and section entitled *Track deformation structures and track infilling*). In the case of the laboratory tracks, the deformation could not be transmitted further downward as the plastic rod penetrated until it almost reached the bottom of the tank.

Another striking similarity observed in both studied human and laboratory tracks is the small depression overlying the *syn-track*

sediments, and that corresponds to the only space available for being filled by *post-track* sediments inside the tracks (yellow dotted lines in Figs 5 and 6, and yellow arrows in Fig. 8D to F). Cross-sections of both human and laboratory tracks also revealed how the structures produced during the penetration and withdrawal (marginal folds and upward deformed layers, respectively) and those produced during their infilling could vary laterally within the same track. This lateral variation, recorded for the first time in this work, is especially remarkable in the cross-sections of the human tracks due to the complexity of the footstep dynamics (Figs 5 and 9), rather than in the laboratory tracks, which were made following a simple vertical trajectory. In the human track, the withdrawal-induced upward deformations are only present in the posterior and anterior cross-sections (sections A–A', D–D' and E–E' in Figs 5 and 9), indicating that the suction effect was more prominent in the area of the heel and the toes. Cross-sections also show how sediments display different degrees of compression. The sediments of the LMMS and the basal sandy layer (S) of the UMMS get thinner in the anterior and posterior cross-sections (sections A–A' to B–B' and D–D' to E–E' in Fig. 5, respectively, and Fig. 9), while they have completely vanished in the central cross-section (section C–C' in Figs 5 and 9). This indicates that the metatarsal of the foot exerted a greater pressure during the track-making process with respect to the heel and the toes. On the other hand, the anterior cross-section shows evidence of a shift in the weight distribution of the foot, as the sediments of the LMMS display different degrees of deformation from the left to the right part of the track (section B–B' in Fig. 5). In addition, cross-sections also reveal the asymmetry of the collapsing process along the track. The sediment collapsed from both walls in its central and posterior parts (sections C–C' to E–E' in Fig. 5) and only from the right wall in its anterior part (section B–B' in Fig. 5). Cross-sections additionally show how the sediment was deformed upward in its anterior part when it was pushed outside of the track during its withdrawal (sections A–A' and B–B' in Figs 5 and 9). Nevertheless, the great lateral variability of sedimentary structures observed between cross-sections implies that incorrect interpretations can be made in the fossil record, where different sections of the same track are not typically observed. This is the case for the most anterior cross-section A–A', which

shows some horizontal layers above the sediments of the LMMS that have been interpreted to be compressed by the toes and afterwards rebounded during their withdrawal (see blue arrows in section A–A' in Fig. 5). If this was the only cross-section to crop out from a fossil track, the horizontal layers could be erroneously interpreted as sediments deposited during the subsequent tides, after the track was made, and not as part of the *syn-track infilling*.

In the case of the laboratory tracks, cross-sections show a minor lateral variation of the structures (Fig. 8D to F), as they were made following a simple vertical trajectory with no horizontal component. This produces upward deformation structures along the entire track (Fig. 8D to F), which contrasts with the human tracks (see sections A–A', D–D' and E–E' in Fig. 5). The main lateral variation observed in the laboratory tracks is that the upward deformation structures developed preferentially in the lower and lateral parts of tracks, while the liquefied infill mostly developed in the central part (Fig. 8D to F).

Finally, another interesting aspect to highlight is that in both human and laboratory tracks, the final width of the tracks in cross-section is narrower than the width of the foot or the plastic rod that made them. This reduction of track width is produced when the water saturated sediments located in the track walls are released from the pressure exerted by the foot or the plastic prism during their withdrawal (see Videos S2 and S3 of laboratory tracks). This implies that neither the width nor the length of the tracks made in semi-liquid sediments can be used to directly infer the foot size of the track-maker and, thus, to interpret other parameters that are estimated from the size of tracks, such as the hip height, which is commonly used, together with the stride length, to obtain the speed of walking (Alexander, 1976; Thulborn, 1990; Marchetti *et al.*, 2019).

Conditions of vertebrate track preservation in semi-liquid sediments

Considering that semi-liquid sediment may be prone to be easily reworked by tides, one might assume that the preservation potential of vertebrate tracks in such sediments is very low, if not null. Nevertheless, the observations herein demonstrate that tracks are potentially well-preserved. In the tide-dominated study site, experiments show that the preservation

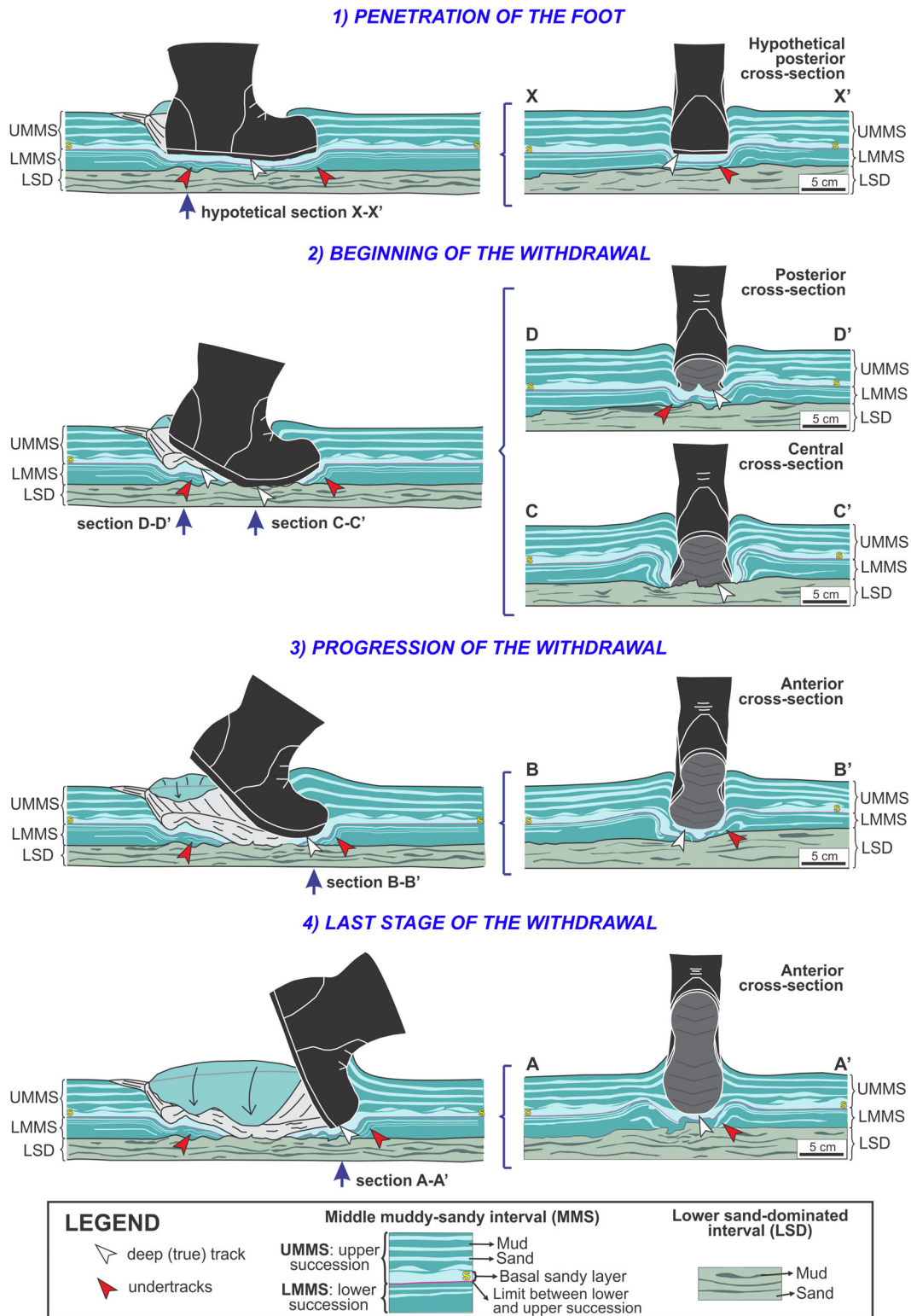


Fig. 9. Reconstruction of the phases of penetration and withdrawal of the human foot within the semi-liquid sediments. Left panel shows longitudinal sections (boot seen from the side) and right panel shows transverse sections (boot seen from behind). Note the lateral variation of the sedimentary structures produced from the anterior to posterior cross-sections as a consequence of the different pressures exerted by the different parts of the foot when walking. White and red arrows indicate the position of the deep (true) track and the undertracks, respectively.

potential of tracks in semi-liquid sediment is strongly dependent on the moment when they are made with respect to the fortnightly tidal cycle. The monitored human track was made one day after the peak of a very high spring tide period (Fig. 4A and B). Afterwards, it was subsequently flooded and filled by sediment (*post-track infilling*) during tides of progressively decreasing energy (Fig. 4A and C). If the track had been made before the spring tide period peak, it probably would have undergone severe erosion during the subsequent tides of progressively increasing energy until the peak. After being almost filled during the descending phase of a spring tide period, the track underwent a period of emersion during the next neap tides, favouring track-bearing sediment desiccation and consolidation (Fig. 4A and C). These processes prevented erosion by the next spring tides that were, additionally, of moderate tidal range (Fig. 4A). During these spring tides, the track got completely covered by sediments (see track in Fig. 4D). Desiccation and consolidation continued during the following neap tides; thus, the next spring tides flooding the site, despite being of high energy, induced only a moderate erosion of the uppermost part of the track-bearing sediments. Erosion was subsequently followed by deposition of a sedimentary succession that sealed ‘*definitively*’ the track with its *syn-track* and *post-track infills* almost totally intact (Fig. 5). Thus, these field experiments demonstrate that, in tidal flat environments, the moment of track impression with respect to tidal cycles and dynamics is a critical condition for tracks to be preserved in semi-liquid sediments.

Identifying true tracks, undertracks and overtracks in semi-liquid sediments

The identification of true tracks, undertracks and overtracks in fossil vertebrate tracks is crucial for making palaeoecological, palaeoenvironmental and palaeoichnological analyses (e.g. Thulborn, 1990; Lockley, 1991; Milàn, 2006; Milàn & Bromley, 2006, 2008; Marty *et al.*, 2009; Díaz-Martínez *et al.*, 2018). Among these, the recognition of true tracks is of great importance, because they represent the surface where the track was made (Lockley, 1991) and, thus, they could record the impressions of the anatomical details left by the track-maker (Leonardi, 1997; Marty *et al.*, 2009). Nevertheless, in vertebrate tracks made in semi-liquid sediments, in which the anatomical fidelity (*sensu* Gatesy &

Falkingham, 2017) is less probable due to the low consistency of sediment (Allen, 1997; Gatesy *et al.*, 1999; Milàn, 2006; Marty *et al.*, 2009), the identification of the true track could be challenging. Its identification would be especially difficult if only the plan view of the tracks is observed in the fossil record. As seen in this study (Figs 3B to F and 8A to C, respectively), the general appearance of field and laboratory tracks in plan view corresponds to a small depression displaying a poorly defined morphology. Moreover, they could show drag marks at their anterior and/or posterior parts. These features in plan view could lead to misinterpreting the tracks as weathered or modified true tracks, that is, as tracks that: “have been modified by erosional processes” (Marty *et al.*, 2016, p. 400).

Although the plan view does not allow to identify the true track, its recognition could be possible in cross-section. As observed in the cross-sections of both human and laboratory tracks, the foot or plastic rod penetrate several centimetres into the semi-liquid sediment until they reach a firmer surface and are later filled by collapsed or liquefied sediment during and after withdrawal (Fig. 9). Thus, the surface that separates the collapsed and/or liquefied sediments from the underlying ones (white arrows in Fig. 9) is the surface that was in contact with the foot (or plastic rod) and, thus, it would correspond to the true track (*sensu* Lockley, 1991) or to the deep track defined by Gatesy (2003), when applied to tracks sinking into soft mud. Gatesy (2003) uses the term deep track for the true tracks that are located within the sediment, as they are overlain by the sediments that have collapsed during and after the withdrawal. For this reason, in the present work, the true track can be named deep track, *sensu* Gatesy (2003). In the studied human track, the deep track is located at different heights within the sediment, as the different parts of the foot had a different degree of penetration (see white arrows in Fig. 9). In the anterior and posterior cross-sections, where the foot penetrated less, the sediment that was in contact with the foot (that is, the deep track) corresponds to the sandy basal layer (S) of the UMMS, which was plastically compressed by the foot together with the underlying sediments and which was later covered by the semi-liquid sediment that collapsed into the track (see anterior and posterior cross-sections in Figs 5 and 9). In the central cross-section, where the foot penetrated deeper, the position

of the deep track is located in the contact with the LSD, as the basal sandy layer (S) of the UMMS and the sediments of the LMMS had completely vanished (see section C–C' of Figs 5, 6 and 9). Therefore, the position of the deep track in the cross-sections corresponds to the surface located in the contact between the sandy basal layer (S) of the UMMS or the sediments of the LSD with the overlying collapsed sediments (Fig. 5). Variations in the position of the deep track within cross-sections clearly reflect the different depths reached by the foot within the sediment during the track-making. As already stated by Avanzini (1998) and Gatesy (2003), the analysis of the distribution of the deformation structures produced by a track and the position of the deep track can provide valuable information about the foot motion within the sediment rather than the anatomical details of the track-maker (i.e. plantar morphology, impressions of the skin, claws or pads, among others).

In the case of the laboratory tracks, the exact position of the deep track is very difficult to identify or delimit as the track-making and withdrawal processes resulted in the complete liquefaction of sediment (Fig. 8D to F).

The identification of undertracks, that is, the transmitted tracks formed by compression of the laminated sediment located below the true track, is critical as well (Thulborn, 1990; Lockley, 1991). Vertebrate tracks executed in experimental flumes have shown that undertracks can be formed under water-saturated sediments and that they display different features according to the composition of the substrate. For example, Milàn & Bromley (2006, 2008) showed how undertracks formed in semi-liquid layered concrete could, in some cases, reflect more anatomical details of the track-maker than the true track, such as the impressions of the digits. Experiments conducted by Jackson *et al.* (2009, 2010) revealed how the undertracks made in semi-liquid homogeneous sand just reflect the general shape of the track but are transmitted much deeper in the sediment. In other cases, in which the sediment shows variations of sediment consistency with depth, undertracks have been described as well. For instance, polished slabs of a Lower Jurassic theropod track reveal the occurrence of well-defined undertracks in stiffer sediments located below the semi-liquid sediment in which the track was made (Avanzini, 1998). Similarly, in the case of the studied human tracks, which were made in a heterolithic muddy and sandy sediment with an

increasing consistency with depth, undertracks were only formed within the sediments of the LMMS that were plastically compressed by the foot at its anterior and posterior parts (see red arrows in Fig. 9). Undertracks were not transmitted further downward into sediments of the LSD, which had a greater consistency and, thus, impeded the downward propagation of deformation (Figs 5 and 9). Undertracks show the general shape of the shod foot and imitate the morphology displayed by the deep track. In the case of the laboratory tracks, undertracks were not formed, as the sediments located below the tracks overlie the base of the flume tank, which impeded the downward transmission of the deformation (Fig. 8D to F).

Finally, overtracks correspond to the sediment that fills the track after the track-making process (e.g. Sung *et al.*, 2001; Marty *et al.*, 2009). For tracks made in semi-liquid sediments, the present experiments demonstrate that overtracks, which correspond to the *post-track infill*, are very poorly developed (see yellow arrows in Figs 5 and 8).

Criteria for recognition of vertebrate tracks made in semi-liquid sediments and for distinction from other soft-sediment deformation structures

The experiments herein have revealed that vertebrate tracks made in semi-liquid sediments display some distinctive structures. Thus, their recognition in ancient counterparts could be used to identify this type of track in the fossil record and to draw conclusions with respect to sediment water content during the track-making process. For this purpose, the human and laboratory tracks were compared with those made by other vertebrates (i.e. sheep, dogs and tourists), which are commonly preserved in upper intertidal sediments of the inner estuary of the BMSM (Fig. 10). Some of these preserved vertebrate tracks display the following features: (i) marginal folds at both sides mostly infilled by liquefied or collapsed sediment (pink arrows and red arrows, respectively, in Fig. 10A to C); (ii) upward deformation structures produced during foot withdrawal (orange arrows in Fig. 10B); and (iii) *post-track infilling*, made up of laminated or structureless sediments (Fig. 10A to C). These features strongly resemble those observed in the field and laboratory experiments, indicating that many vertebrate tracks preserved in these upper intertidal sediments

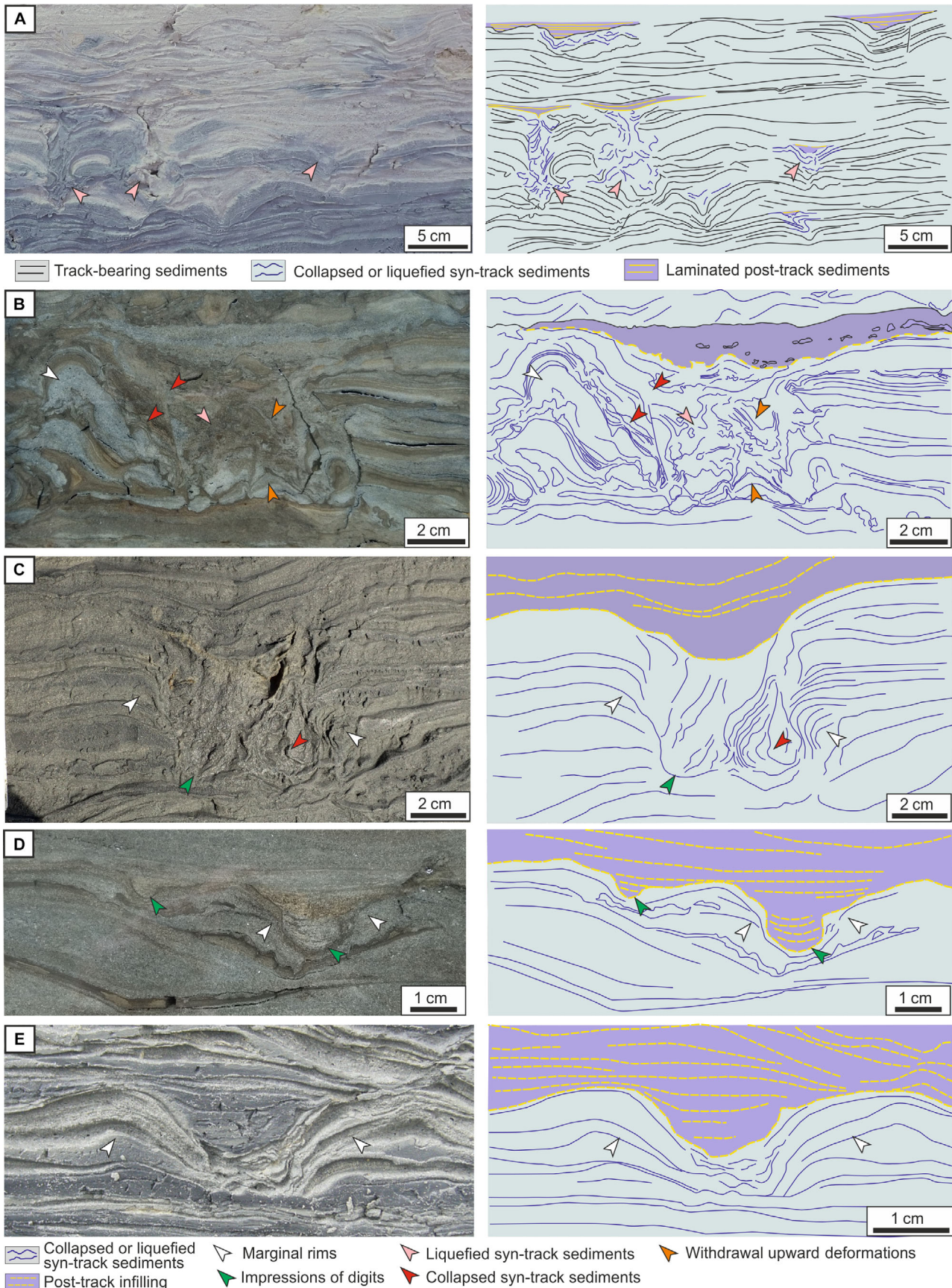


Fig. 10. Field photographs (to the left) and line drawings (to the right) of vertebrate tracks preserved in the recent upper intertidal sediments of the Bay of Mont-Saint-Michel. (A) Sediments deformed by sheep tracks. Tracks are very deep and show collapsed or liquefied features in the lower-left part of the outcrop, indicating that they were made in water-saturated sediments. Tracks are progressively shallower and include less collapsed or liquefied features to the right and to the upper part, indicating that they were made in sediments that gradually had less water content. (B) and (C) Sheep tracks made in semi-liquid sediments. Both tracks show marginal folds (white arrows) at both sides and are filled by liquefied and/or collapsed sediments (pink and red arrows, respectively). Track of Fig. 10C also displays the impressions of digits at its lowermost part (green arrow). In both cases, the uppermost part of the tracks is filled by structureless or laminated *post-track* sediments, deposited during subsequent flooding by tides. (D) and (E) Sheep tracks made in sediments with low to moderate water content. Note that tracks are directly infilled by laminated *post-track* sediments. Track of Fig. 10D preserves the impressions of both digits (green arrows).

were made in semi-liquid sediments. Some of these tracks may also display the impressions of the digits below the *syn-track infilling*, indicating that the underlying sediment had a greater consistency (green arrow in Fig. 10C). Other preserved tracks may also display marginal folds at both sides and may preserve the impressions of digits, but they lack collapsed and/or liquefied sediments and are exclusively filled by *post-track* laminated sediments (Fig. 10A, D and E), indicating that no liquefaction or collapsing processes occurred during the track-making, probably due to the low water content of the sediment. Therefore, the recognition in fossil vertebrate tracks of both *syn-track* and *post-track infillings* and withdrawal-induced upward deformation structures could allow to identify tracks made in semi-liquid sediments.

A striking aspect that arises when analysing the vertebrate tracks made in semi-liquid sediments in the BMSM, is their resemblance to other soft-sediment deformation structures (SSDS), especially to convolute bedding and/or

balls-and-pillows triggered by earthquakes (Berra & Felletti, 2011; Moretti & van Loon, 2014), overloading (van Loon, 2009), tidal bores (Tessier & Terwindt, 1994; Greb & Archer, 2007; Fan *et al.*, 2014; Tessier *et al.*, 2017) and storm waves (Alfaro *et al.*, 2002), among others. This similarity is especially remarkable when sediments appear highly distorted by abundant vertebrate tracks (Fig. 11). For example, convolute bedding commonly comprises folds with wide 'synclines' and narrow 'anticlines' (e.g. McKee *et al.*, 1967; Allen, 1982; Collinson & Thompson, 1984; Singh & Bhardwaj, 1991; Greb & Archer, 2007; Çiner *et al.*, 2012; Tessier *et al.*, 2017), which could resemble the track depression and the marginal folds that characteristically develop in tracks made in semi-liquid sediments (Figs 5, 6, 8D, 8E, 10B and 10C) and in sediments with less water content (Fig. 10D and E). Vertebrate tracks could be also misinterpreted as balls-and-pillows because they typically display wide concave-upward morphologies (e.g. Montenat *et al.*, 2007; Moretti & Sabato, 2007; van Loon, 2009; Berra & Felletti,



Fig. 11. Field photograph of some upper intertidal sediments of the Bay of Mont-Saint-Michel that are highly deformed by human tracks (white arrows). Note that tracks resemble other soft-sediment deformation structures, such as convolute bedding and/or balls-and-pillows.

2011; Moretti & van Loon, 2014), which resemble the general shape of tracks in cross-section (Figs 5, 6, 8D, 8E, 10B and 10C). Nevertheless, despite the morphological resemblance between these structures, vertebrate tracks are limited to the size of the autopodia of the track-maker, the largest ones known being made by sauropod dinosaurs up to 1.30 m wide (e.g. Lee & Lee, 2006; Lockley *et al.*, 2007; Boutakiout *et al.*, 2020), whereas convolute bedding and balls-and-pillows could be even wider, especially when they are triggered by earthquakes, which could reach several metres in width (e.g. Alfaro *et al.*, 2010). Other similarities observed in these structures are that balls-and-pillows and convolute bedding are commonly associated with highly distorted levels caused by the liquefaction of sediment (Bordy & Catuneanu, 2002; Montenat *et al.*, 2007; Moretti & Sabato, 2007; Berra & Felletti, 2011), which could have a similar appearance to the liquefied *syn-track* sediments that infill some tracks (Figs 8D, 8E, 10A and 10B).

Some features that have been used in the literature to differentiate vertebrate tracks from convolute bedding and balls-and-pillows, especially those triggered by earthquakes, is their lateral extent. Vertebrate tracks show a discontinuous distribution in many outcrops (Loope, 1986; Melchor, 2015), whereas the other two types of SSDS commonly show a regular distribution that can be followed over great lateral extensions (hundreds of metres to kilometres; Moretti & van Loon, 2014; Varejao *et al.*, 2022). Nevertheless, caution should be taken with this assumption, because vertebrate tracks can be followed along significant distances (hundreds of metres) when they occur in vertebrate trackways (e.g. Meyer, 1993; Santos, 1996; Marty *et al.*, 2003; Cobos *et al.*, 2016; Razzolini *et al.*, 2016; Campos-Soto *et al.*, 2017, 2019; Lockley & Meyer, 2022). Moreover, some convolute bedding and balls-and-pillows, especially those associated with overloading, can also show limited extensions because they may be constrained to specific facies (e.g. McKee *et al.*, 1967; Díaz-Molina, 1979; Çiner *et al.*, 2012) and, thus, the criteria based on lateral extension are not useful in these cases.

Sedimentological interpretations could also provide useful information for differentiation of vertebrate tracks and the other types of SSDS. While vertebrate tracks are typically constrained to very shallow settings, especially those subject to subaerial exposure, convolute bedding and

balls-and-pillows can develop in a wide range of very shallow to deep environments. Thus, if the analysed structures occur in deep water deposits, vertebrate tracks can be ruled out. However, if the structures occur in shallow facies, additional criteria are necessary. In this regard, one key aspect that could be useful is to evaluate the lateral and vertical distribution of the SSDS. In contrast to convolute bedding and balls-and-pillows, vertebrate tracks made in semi-liquid sediments may be laterally and vertically associated with other tracks made in sediments containing less water content, which penetrate less in the sediment, show a better definition of the shape and are exclusively filled by *post-track* laminated sediments, as observed in the recent tidal sediments of the BMSM (Fig. 10A). Another fundamental aspect to consider for differentiating these SSDS, is their internal structure. For example, convolute bedding and balls-and-pillows internally display concave-upward laminae that are conformable to their basal shape (McKee *et al.*, 1967; Alfaro *et al.*, 1997; Gehling, 2000; Greb & Archer, 2007; Deev *et al.*, 2009; van Loon, 2009; Berra & Felletti, 2011; Çiner *et al.*, 2012; Bizhu & Xiufu, 2015; Al-Muffi & Arnott, 2020). This internal structure contrasts with that observed in the studied vertebrate tracks infilled by collapsed sediment, which is characteristically formed by layers that are deformed downward (Figs 5, 6, 10B and 10C). Furthermore, in contrast to convolute bedding and balls-and-pillows, vertebrate tracks made in semi-liquid sediments display internal cross-cutting surfaces (see Figs 5 and 6; white arrows in Figs 9 and 10A to C). Moreover, vertebrate tracks may be filled by layers of sediment that are folded in opposite directions, such as the downward deformed layers that are displayed by the collapsed sediment and the upward deformation structures produced during foot withdrawal (see red and green arrows, respectively in Fig. 5). More importantly, another aspect that is exclusive to vertebrate tracks is that anatomical details, such as the impressions of digits, may be present below the *syn-track infilling* in some tracks (see green arrow in Fig. 10C).

CONCLUSIONS

The consecutive cross-sections of a human track made in tidal sediments and monitored until its complete burial, and the comparison with those

of a track made in a flume tank, have allowed to understand the mechanisms of formation and preservation of vertebrate tracks made in semi-liquid sediment.

- Both field and laboratory tracks comprise the following diagnostic sedimentary structures that reproduce with great fidelity their mechanisms of formation and infilling: (i) marginal folds that develop at both sides of tracks during the penetration of the foot; (ii) some upward deformed structures produced during its withdrawal; (iii) a *syn-track infilling*, which almost entirely fills the tracks during and right after withdrawal of the foot, formed by sediment that collapses from the tracks walls or by liquefied sediment; and (iv) a *post-track infilling* that completes the infilling of the tracks during their subsequent flooding.

- The consecutive cross-sections made in these tracks allow to reproduce the foot motion within the sediment, as the position of the deep (true) track varies along the same track depending on the different pressures exerted from the posterior to the anterior parts of the foot. The complex footstep dynamics also makes the structures generated during the track formation and infilling vary laterally within the same track.

- This study shows that vertebrate tracks made in semi-liquid sediments have a much higher preservation potential in the fossil record than previously considered. In tidal settings, their preservation is optimal if they are made after the peak of a spring tide period and undergo desiccation and consolidation during neap tides, which prevents their erosion and favours their complete burial by sediments.

- The identification of these tracks in ancient successions (using the diagnostic structures described here) provides valuable palaeoenvironmental information, as it allows: (i) to discriminate them from other vertebrate tracks made in sediments with less water content, which lack collapsed and/or liquefied sediments in their infill and are exclusively filled by *post-track* sediments; and (ii) to distinguish them from other soft-sediment deformation structures (SSDS), such as convolute bedding and balls-and-pillows, with which they can display strong resemblances. In contrast to the other SSDS, vertebrate tracks made in semi-liquid sediments display: (i) internal cross-cutting surfaces; (ii) withdrawal-induced upward deformation structures; and (iii) impressions of digits; and occur

in very shallow facies, where tracks may be laterally and vertically related with other tracks made in sediments with less water content.

ACKNOWLEDGEMENTS

This research was funded by the projects PGC2018-094034-B-C21 and PID2022-136717NB-I00 of the Spanish Ministry of Science and Innovation. Authors also thank the support of the M2C Laboratory (CNRS-Université de Caen Normandie) and the “Sedimentary Geology, Paleoclimate and Environmental Change” UCM Research Group (Ref. 910198). SCS was supported with a postdoctoral fellowship of the Université de Caen Normandie. The authors would like to thank Drs Jens N. Lallensack and Matteo Belvedere for their reviews, as well as Gabriela Mángano (Chief Editor) and Massimiliano Ghinassi (Associate Editor) for their advice and comments, which improved the quality and clarity of the manuscript. We are also grateful to Dr Sandric Lesourd for helping us with sampling the sediments for the flume experiments, Laia Real, Elena Ojeda and Armelle Decaulne for their help on the field, and Juan Carlos Salamanca, Beatriz Moral and Aitor Antón for the great effort carried out during the preparation of samples and their laboratory support.

CONFLICT OF INTEREST

The authors have no conflicts of interest to declare.

DATA AVAILABILITY STATEMENT

The data that support the findings of this study are available from the corresponding author upon reasonable request.

REFERENCES

- Alcalá, L., Pérez-Lorente, F., Luque, L., Cobos, A., Royo-Torres, R. and Mampel, L. (2014) Dinosaur footprints in shallowing intertidal deposits of the Jurassic-Cretaceous transition in the Iberian Range (Teruel, Spain). *Ichnos*, **2**, 19–31.
- Alexander, R.M.N. (1976) Estimates of speeds of dinosaurs. *Nature*, **261**, 129–130.
- Alexander, R.M.N. (2004) Bipedal animals, and their differences from humans. *J. Anat.*, **204**, 321–330.

- Alfaro, P., Moretti, M. and Soria, J.M.** (1997) Soft-sediment deformation structures induced by earthquakes (seismites) in pliocene lacustrine deposits (Guadiz-Baza Basin, Central Betic Cordillera). *Eclogae Geol. Helv.*, **90**, 531–540.
- Alfaro, P., Delgado, J., Estévez, A., Molina, J.M., Moretti, M. and Soria, J.M.** (2002) Liquefaction and fluidization structures in Messinian storm deposits (Bajo Segura Basin, Betic Cordillera, southern Spain). *Int. J. Earth Sci.*, **91**, 505–513.
- Alfaro, P., Gibert, L., Moretti, M., García-Tortosa, F.J., Sanz de Galdeano, C., Galindo-Zaldívar, J. and López-Garrido, A.C.** (2010) The significance of giant seismites in the Plio-Pleistocene Baza palaeo-lake (S Spain). *Terra Nova*, **22**, 172–179.
- Allen, J.R.L.** (1982) *Sedimentary Structures: Their Character and Physical Basis*, p. 593. Elsevier, Amsterdam.
- Allen, J.R.L.** (1997) Subfossil mammalian tracks (Flandrian) in the Severn Estuary, S.W. Britain: mechanics of formation, preservation and distribution. *Philos. Trans. R. Soc. B*, **352**, 481–518.
- Al-Muffi, O.N. and Arnott, W.C.** (2020) The origin and significance of convolute lamination and pseudonodules in an ancient deep-marine turbidite system: from deposition to diagenesis. *J. Sediment. Res.*, **90**, 480–492.
- Avanzini, M.** (1998) Anatomy of a footprint: Bioturbation as a key to understanding dinosaur walk dynamics. *Ichnos*, **63**, 129–139.
- Avanzini, M., Piñuela, L. and García-Ramos, J.C.** (2012) Late Jurassic footprints reveal walking kinematics of theropod dinosaurs. *Lethaia*, **45**, 238–252.
- Bajard, J.** (1966) Figures et structures sédimentaires dans la zone intertidale de la partie orientale de la Baie du Mont Saint-Michel. *Revue de géologie dynamique et de géographie physique*, **8**, 39–111.
- Berra, F. and Felletti, F.** (2011) Syndepositional tectonics recorded by soft-sediment deformation and liquefaction structures (continental Lower Permian sediments, Southern Alps, Northern Italy): Stratigraphic significance. *Sedimentary Geol.*, **235**, 249–263.
- Billeaud, I.** (2007) *Dynamique de construction d'un prisme sédimentaire littoral en régime mégatidal (la Baie du Mont-Saint-Michel). Interfaces continentales, environnement*, p. 239. Université de Caen, Caen.
- Billeaud, I., Tessier, B., Lesueur, P. and Caline, B.** (2007) Preservation potential of highstand coastal sedimentary bodies in a macrotidal basin: Example from the Bay of Mont-Saint-Michel, NW France. *Sedimentary Geol.*, **202**, 754–775.
- Bizhu, H. and Xiufu, Q.** (2015) Advances and overview of the study on paleo-earthquake events: a review of seismites. *Acta Geol. Sin.*, **89**, 1702–1746.
- Bonnot-Courtois, C.** (2012) Dynamique sédimentaire intertidale en baie du Mont-Saint-Michel entre évolution naturelle et aménagements. In: *XIIèmes Journées Nationales Génie Côtier Génie Civil*, pp. 187–222. Editions Paralia CFL, Cherbourg.
- Bordy, E.M. and Catuneanu, O.** (2002) Sedimentology of the Beaufort-Molteno Karoo fluvial strata in the Tuli Basin, South Africa. *S. Afr. J. Geol.*, **105**, 51–66.
- Bourcart, J. and Charlier, R.** (1959) The tangué: a “nonconforming” sediment. *Bull. Geol. Soc. Am.*, **70**, 565–568.
- Boutakiout, M., Masrou, M. and Pérez-Lorente, F.** (2020) New sauropod morphotype definition in the oriental section 0F Imilchil megatracksite, high atlas (Morocco). *J. Afr. Earth Sci.*, **161**, 103664.
- Brand, L. and Tang, T.** (1991) Fossil vertebrate footprints in the Coconino Sandstone (Permian) of northern Arizona: Evidence for underwater origin. *Geology*, **19**, 1201–1204.
- Caline, B.** (1982) *Le secteur occidental de la baie du Mont-Saint-Michel. Morphologie, sédimentologie et cartographie de l'estran*, p. 250. Éditions du Bureau de recherches géologiques et minières, Paris.
- Caline, B., L'Homer, A., Marchand, Y., Le Rhun, J., Bonnot-Courtois, C. and Le Vot, M.** (2002) The main morphodepositional units as seen from space. In: *The Bay of Mont-Saint-Michel and the Rance Estuary: Mémoire 26* (Eds Bonnot-Courtois, C., Caline, B., L'Homer, A. and Le Vot, M.), pp. 27–29. Bulletin Centre Recherches Elf Exploration Production, Elf.
- Campos-Soto, S.** (2020) *Estratigrafía, sedimentología y edad de los sistemas costeros del Kimmeridgiense-Titoniense del SE de la cuenca Ibérica: implicación de los nuevos resultados en la correlación de unidades y en la paleogeografía de Iberia*. Thesis Doctoral, p. 342. Universidad Complutense de Madrid, Madrid.
- Campos-Soto, S., Cobos, A., Caus, E., Benito, M.I., Fernandez-Labrador, L., Suarez-Gonzalez, P., Quijada, I.E., Mas, R., Royo-Torres, R. and Alcalá, L.** (2017) Jurassic Coastal Park: A great diversity of palaeoenvironments for the dinosaurs of the Villar del Arzobispo Formation (Teruel, eastern Spain). *Palaeogeogr. Palaeoclimatol. Palaeoecol.*, **485**, 154–177.
- Campos-Soto, S., Benito, M.I., Cobos, A., Caus, E., Quijada, I.E., Suarez-Gonzalez, P., Mas, R., Royo-Torres, R. and Alcalá, L.** (2019) Revisiting the age and palaeoenvironments of the Upper Jurassic-Lower Cretaceous? dinosaur-bearing sedimentary record of eastern Spain: implications for Iberian palaeogeography. *J. Iberian Geol.*, **45**, 471–510.
- Campos-Soto, S., Tessier, B., Mouzéz, D., Benito, M.I., Quijada, I.E. and Suarez-Gonzalez, P.** (2022a) Tidal flats of the Bay of Mont-Saint-Michel: a natural laboratory to understand the sedimentary controls on the formation and preservation of vertebrate tracks. In: *Abstracts 10th International Congress of Tidal Sedimentology*, pp. 55–56. Tidalites, Matera.
- Campos-Soto, S., Tessier, B., Mouzéz, D., Benito, M.I., Quijada, I.E. and Suarez-Gonzalez, P.** (2022b) On the formation and preservation of vertebrate tracks in semi-liquid sediments: new insights from the tidal sediments of the Bay of Mont-Saint-Michel and laboratory-controlled experiments. In: *Abstracts 10th International Congress of Tidal Sedimentology*, pp. 96–97. Tidalites, Matera.
- Cariou, E., Olivier, N., Pittet, B., Mazin, J.M. and Hantzpergue, P.** (2014) Dinosaur track record on a shallow carbonate-dominated ramp (Loulle section, Late Jurassic, French Jura). *Facies*, **60**, 229–253.
- Carvalho, I.S., Leonardi, G., Rios-Netto, A.M., Borghi, L., Freitas, A.P., Andrade, J.A. and Idalécio de Freitas, F.** (2021) Dinosaur trampling from the Aptian of Araripe Basin, NE Brazil, as tools for paleoenvironmental interpretation. *Cretaceous Res.*, **117**, 104626.
- Castanera, D., Vila, B., Razzolini, N.L., Santos, V.F., Pascual, C. and Canudo, J.L.** (2014) Sauropod trackways of the Iberian Peninsula: palaeoetological and palaeoenvironmental implications. *J. Iberian Geol.*, **40**, 49–59.
- Çiner, A., Kosun, E. and Deynoux, M.** (2012) Fluvial, evaporitic and shallow-marine facies architecture,

- depositional evolution and cyclicity in the Sivas Basin (Lower to Middle Miocene), Central Turkey. *J. Asian Earth Sci.*, **2**, 147–165.
- Cobos, A., Gascó, F., Royo-Torres, R. and Lockley, M.G.** (2016) Dinosaur tracks as “four-dimensional phenomena” reveal how different species moved. In: *Dinosaur Tracks: The Next Steps* (Eds Falkingham, P.L., Marty, D. and Richter, A.), pp. 244–256. Indiana University Press, Bloomington.
- Collinson, J.D. and Thompson, D.B.** (1984) *Sedimentary Structures*, p. 194. George Allen & Unwin, London.
- Deev, E.V., Zolnikov, I.D. and Gus'kov, S.A.** (2009) Seismites in Quaternary sediments of southeastern Altai. *Russian Geol. Geophys.*, **50**, 546–561.
- Díaz-Martínez, I., Cónsole-Gonella, C., Valais, S. and Salgado, L.** (2018) Vertebrate tracks from the Paso Cordoba fossiliferous site (Anacleto and Allen formations, Upper Cretaceous), Northern Patagonia, Argentina: Preservational, environmental and palaeobiological implications. *Cretaceous Res.*, **83**, 207–220.
- Díaz-Molina, M.** (1979) Características sedimentológicas de los paleocanales de la unidad detrítica superior al N. de Huete (Cuenca). *Estudios Geológicos*, **35**, 241–251.
- D'Orazi, P., Bernardi, M., Cinquegranelli, A., Santos, V.F.D., Marty, D., Petti, F.M., Caetano, P.S. and Wagensommer, A.** (2016) A review of the dinosaur track record from Jurassic and Cretaceous shallow marine carbonate depositional environments. In: *Dinosaur Tracks: The Next Steps* (Eds Falkingham, P.L., Marty, D. and Richter, D.A.), pp. 381–390. Indiana University Press, Bloomington.
- Duveau, J., Berillon, G. and Verna, C.** (2021) On the tracks of Neandertals: The ichnological assemblage from Le Rozel (Normandy, France). In: *Reading Prehistoric Human Tracks: Methods & Material* (Eds Pastoors, A. and Lenssen-Erz, T.), pp. 183–200. Springer, Cham.
- Falkingham, P.L.** (2014) Interpreting ecology and behaviour from the vertebrate fossil track record. *J. Zool.*, **292**, 222–228.
- Falkingham, P.L., Turner, M.L. and Gatesy, S.M.** (2020) Constructing and testing hypotheses of dinosaur foot motions from fossil tracks using digitization and simulation. *Palaeontology*, **63**, 865–880.
- Fan, D.D., Tu, J., Shang, S. and Cai, G.** (2014) Characteristics of tidal bore deposits and facies associations in the Qiantang estuary, China. *Mar. Geol.*, **348**, 1–14.
- Gatesy, S.M.** (2003) Direct and Indirect Track Features: What Sediment Did a Dinosaur Touch? *Ichnos*, **10**, 91–98.
- Gatesy, S.M. and Falkingham, P.L.** (2017) Neither bones nor feet: Track morphological variation and “preservation quality”. *J. Vertebrate Paleontol.*, **37**, e1314298.
- Gatesy, S.M. and Falkingham, P.L.** (2020) Hitchcock's Leptodactyli, penetrative tracks, and dinosaur footprint diversity. *J. Vertebrate Paleontol.*, **40**, e1781142.
- Gatesy, S.M., Middleton, K.M., Jenkins, F.A. and Shubin, N.H.** (1999) Three-dimensional preservation of foot movements in Triassic theropod dinosaurs. *Nature*, **399**, 141–144.
- Gehling, J.G.** (2000) Environmental interpretation and a sequence stratigraphic framework for the terminal Proterozoic Ediacara Member within the Rawnsley Quartzite, South Australia. *Precambrian Res.*, **100**, 65–95.
- Gerbersdorf, S.U. and Wieprecht, S.** (2015) Biostabilization of cohesive sediments: revisiting the role of abiotic conditions, physiology and diversity of microbes, polymeric secretion, and biofilm architecture. *Geobiology*, **13**, 68–97.
- Graversen, O., Milàn, J. and Loope, D.B.** (2007) Dinosaur Tectonics: A Structural Analysis of Theropod Undertracks with a Reconstruction of Theropod Walking Dynamics. *J. Geol.*, **115**, 641–654.
- Greb, S.F. and Archer, A.W.** (2007) Soft-sediment deformation produced by tides in a meizoseismic area, Turnagain Arm, Alaska. *Geology*, **35**, 435–438.
- Helm, C.W., Lockley, M.G., Cawthra, H.C., De Vynck, J.C., Dixon, M.G., Rust, R., Stear, W., Van Tonder, M. and Zipfel, B.** (2023) Possible shod-hominin tracks on South Africa's Cape coast. *Ichnos*, **30**, 79–97.
- Jackson, S.J., Whyte, M.A. and Romano, M.** (2009) Laboratory-controlled simulations of dinosaur footprints in sand: a key to understanding vertebrate track formation and preservation. *Palaios*, **24**, 222–238.
- Jackson, S.J., Whyte, M.A. and Romano, M.** (2010) Range of experimental dinosaur (*Hypsilophodon foxii*) footprints due to variation in sand consistency: How wet was the track? *Ichnos*, **17**, 197–214.
- Kyparissi-Apostolika, N. and Manolis, S.K.** (2021) Reconsideration of the antiquity of the Middle Palaeolithic footprints from Theopetra Cave (Thessaly, Greece). In: *Reading Prehistoric Human Tracks: Methods & Material* (Eds Pastoors, A. and Lenssen-Erz, T.), pp. 169–182. Springer, Cham.
- Lallensack, J.N., Farlow, J.O. and Falkingham, P.L.** (2022) A new solution to an old riddle: elongate dinosaur tracks explained as deep penetration of the foot, not plantigrade locomotion. *Palaeontology*, **65**, 1–17.
- Lanier, W.P. and Tessier, B.** (1998) Climbing-ripple bedding in the fluvio-estuarine transition: a common feature associated with tidal dynamics (modern and ancient analogues). In: *Tidalites: Processes and Products* (Eds Alexander, C. and Henry, V.J.), *SEPM Spec. Publ.*, **61**, 109–118.
- Larsonneur, C., Auffret, J.P., Caline, B., Gruet, Y., Lautridou, J.P., L'Homer, S.P., Morzadec, M.T., Migniot, C., Nikodic, J., Sornin, J.M. and Tessier, B.** (1989) La baie du Mont-Saint-Michel: un modèle de sédimentation en zone tempérée. *Bulletin de l'Institut de Géologie du Bassin d'Aquitaine*, **46**, 5–73.
- Ledoux, L., Berillon, G., Fourment, N., Muth, X. and Jaubert, J.** (2021) Evidence of the use of soft footwear in the Gravettian cave of Cussac (Dordogne, France). *Sci. Rep.*, **11**, 22727.
- Lee, Y.N. and Lee, H.J.** (2006) A sauropod trackway in Donghae-Myeon, Goseong County, South Gyeongsang province, Korea and its paleobiological implications of Uhangri manus-only sauropod tracks. *J. Paleont. Soc. Korea*, **22**, 1–14.
- Leonardi, G.** (1997) Problemática actual de las icnitas de dinosaurios. *Revista de la Sociedad Geológica de España*, **10**, 341–353.
- L'Homer, A. and Caline, B.** (2002) Hydrodynamic factors. In: *The Bay of Mont-Saint-Michel and the Rance Estuary: Mémoire 26* (Eds Bonnot-Courtois, C., Caline, B., L'Homer, A. and Le Vot, M.), pp. 29–36. Bulletin Centre Recherches Elf Exploration Production, Elf.
- L'Homer, A., Courbouleix, S., Chantraine, J., Deroin, J.P., Bonnot-Courtois, C., Caline, B., Ehrhold, A., Lautridou, J.P. and Morzadec-Kerfourn, M.T.** (1999) *Notice explicative, Carte géologique France (1:50.000), feuille Baie du Mont-Saint-Michel (208)*, p. 184. BRGM, Orléans.
- L'Homer, A., Bonnot-Courtois, C. and Caline, B.** (2002) Distribution of sediments in the intertidal and subtidal zone. In: *The Bay of Mont-Saint-Michel and the Rance Estuary: Mémoire 26* (Eds Bonnot-Courtois, C., Caline, B.,

- L'Homer, A. and Le Vot, M.), pp. 36–43. Bulletin Centre Recherches Elf Exploration Production, Elf.
- Lockley, M.G.** (1986) The paleobiological and palaeoenvironmental importance of dinosaur footprints. *Palaios*, **1**, 37–47.
- Lockley, M.G.** (1991) *Tracking Dinosaurs. A New Look to an Ancient World*, p. 238. Cambridge University Press, Cambridge.
- Lockley, M.G.** and **Meyer, C.A.** (2022) The megatracksite phenomenon: implications for tetrapod palaeobiology across terrestrial-shallow-marine transitional zones. In: *Ichnology in Shallow-Marine and Transitional Environments* (Eds Cónsole-Gonella, C., de Valais, S., Díaz-Martínez, I., Citton, P., Verde, M. and McIlroy, D.), *Geol. Soc. Spec. Publ.*, **522**, 1–40.
- Lockley, M.G., Lires, J., García-Ramos, J.C., Piñuela, L. and Avanzini, M.** (2007) Shrinking the World's Largest Dinosaur Tracks: Observations on the Ichnotaxonomy of *Gigantosauropus asturiensis* and *Hispanosauropus hauboldi* from the Upper Jurassic of Asturias, Spain. *Ichnos*, **14**, 247–255.
- Loope, D.B.** (1986) Recognizing and utilizing vertebrate tracks in cross section: Cenozoic hoofprints from Nebraska. *Palaios*, **1**, 141–151.
- Manning, P.L.** (2004) A new approach to the analysis and interpretation of tracks: examples from the dinosaurian. In: *The Application of Ichnology to Palaeoenvironmental and Stratigraphic Analysis* (Ed McIlroy, D.), *Geol. Soc. Spec. Publ.*, **228**, 93–123.
- Marchetti, L., Belvedere, M., Voigt, S., Klein, H., Castanera, D., Diaz-Martínez, I., Marty, M., Xing, L., Feola, S., Melchor, R.N. and Farlow, J.O.** (2019) Defining the morphological quality of fossil footprints. Problems and principles of preservation in tetrapod ichnology with examples from the Palaeozoic to the present. *Earth Sci. Rev.*, **193**, 109–145.
- Marty, D.** (2008) *Sedimentology, Taphonomy, and Ichnology of Late Jurassic Dinosaur Tracks from the Jura Carbonate Platform (Chevenez-Combe Ronde Tracksite, NW Switzerland): Insights into the Tidal-Flat Palaeoenvironment and Dinosaur Diversity, Locomotion, and Palaeoecology*. Ph.D. Thesis, p. 278. University of Fribourg, Fribourg.
- Marty, D., Wolfgang, A.H., Iberg, A., Calvin, L., Meyer, C. and Lockley, M.G.** (2003) Preliminary Report on the Courtedoux Dinosaur Tracksite from the Kimmeridgian of Switzerland. *Ichnos*, **10**, 209–219.
- Marty, D., Meyer, C.A. and Billon-Bruyat, J.P.** (2006) Sauropod trackway patterns expression of special behaviour related to substrate consistency? An example from the Late Jurassic of northwestern Switzerland. *Hantkeniana*, **5**, 38–41.
- Marty, D., Strasser, A. and Meyer, C.A.** (2009) Formation and Taphonomy of Human Footprints in Microbial Mats of Present-Day Tidal-flat Environments: Implications for the Study of Fossil Footprints. *Ichnos*, **16**, 127–142.
- Marty, D., Falkingham, P.L. and Richter, A.** (2016) Dinosaur Track Terminology: A Glossary of Terms. In: *Dinosaur Tracks – the Next Steps* (Eds Falkingham, P., Marty, D. and Richter, A.), pp. 309–402. Indiana University Press, Bloomington.
- McKee, E.D., Crosby, E.J. and Berryhill, H.I.** (1967) Flood deposits, Bijou Creek, Colorado, June 1965. *J. Sediment. Petrol.*, **37**, 829–851.
- Melchor, R.N.** (2015) Application of vertebrate trace fossils to palaeoenvironmental analysis. *Palaeogeogr. Palaeoclimatol. Palaeoecol.*, **439**, 79–96.
- Meyer, C.A.** (1993) A sauropod dinosaur megatracksite from the Late Jurassic of northern Switzerland. *Ichnos*, **3**, 29–38.
- Milà, J.** (2006) Variations in the morphology of emu (*Dromaius novaehollandiae*) tracks reflecting differences in walking pattern and substrate consistency: ichnotaxonomic implications. *Palaeontology*, **49**, 405–420.
- Milà, J. and Bromley, R.G.** (2006) True tracks, undertracks and eroded tracks, experimental work with tetrapod tracks in laboratory and field. *Palaeogeogr. Palaeoclimatol. Palaeoecol.*, **231**, 253–264.
- Milà, J. and Bromley, R.G.** (2008) The Impact of Sediment Consistency on Track and Undertrack Morphology: Experiments with Emu Tracks in Layered Cement. *Ichnos*, **15**, 18–24.
- Milà, J., Clemmensen, L.B. and Bonde, N.** (2021) Vertical sections through dinosaur tracks (Late Triassic lake deposits, East Greenland)-undertracks and other subsurface deformations structures revealed. *Lethaia*, **37**, 285–296.
- Montenat, C., Barrier, P., Ott d'Estevou, P. and Hibsich, C.** (2007) Seismites: An attempt at critical analysis and classification. *Sedimentary Geol.*, **196**, 5–30.
- Moretti, M. and Sabato, L.** (2007) Recognition of trigger mechanisms for soft-sediment deformation in the Pleistocene lacustrine deposits of the Sant'Arcangelo Basin (Southern Italy): Seismic shock vs. overloading. *Sedimentary Geol.*, **196**, 31–45.
- Moretti, M. and van Loon, A.J.** (2014) Restrictions to the application of 'diagnostic' criteria for recognizing ancient seismites. *J. Palaeogeogr.*, **3**, 162–173.
- Quijada, I.E., Suarez-Gonzalez, P., Benito, M.I. and Mas, R.** (2013) New insights on stratigraphy and sedimentology of the Oncala Group (eastern Cameros Basin): implications for the paleogeographic reconstruction of NE Iberia at Berriasian times. *J. Iberian Geol.*, **39**, 313–334.
- Quijada, I.E., Suarez-Gonzalez, P., Benito, M.I. and Mas, R.** (2016) Tidal versus continental sandy-muddy flat deposits: evidence from the Oncala Group (Early Cretaceous, N Spain). In: *Contributions to Modern and Ancient Tidal Sedimentology* (Eds Tessier, B. and Reynaud, J.-Y.), *IAS Spec. Publ.*, **47**, 133–159.
- Razzolini, N.A., Oms, O., Castanera, D., Vila, B., Faria dos Santos, V. and Galobart, A.** (2016) Ichnological evidence of Megalosaurid Dinosaurs Crossing Middle Jurassic Tidal Flats. *Sci. Rep.*, **6**, 31494.
- Santos, V.F.** (1996) A new sauropod tracksite from the Middle Jurassic of Portugal. *Gaia*, **10**, 5–13.
- Singh, A. and Bhardwaj, B.D.** (1991) Fluvial facies model of the Ganga River sediments, India. *Sediment. Geol.*, **72**, 135–146.
- Stal, L.J.** (2012) Cyanobacterial Mats and Stromatolites. In: *Ecology of Cyanobacteria II: Their Diversity in Space and Time* (Ed Whitton, B.A.), pp. 65–125. Springer, Dordrecht.
- Sung, P., Joo Kim, I. and Lee, Y.** (2001) Dinosaur track-bearing deposits in the Cretaceous Jindong Formation, Korea: occurrence, palaeoenvironments and preservation. *Cretaceous Res.*, **22**, 79–92.
- Tessier, B.** (1993) Upper intertidal rhythmites in the Mont-Saint-Michel Bay (NW France): Perspectives for paleoreconstruction. *Mar. Geol.*, **110**, 355–367.

- Tessier, B.** (2002) The depositional facies of the inner estuary: the tidal rhythmites in the tangles at Gué de l'Épine. In: *The Bay of Mont-Saint-Michel and the Rance Estuary: Mémoire 26* (Eds Bonnot-Courtois, C., Caline, B., L'Homer, A. and Le Vot, M.), pp. 82–89. Bulletin Centre Recherches Elf Exploration Production, Elf.
- Tessier, B.** and **Terwindt, J.H.J.** (1994) Un exemple de déformations synsédimentaires en milieu intertidal: l'effet du mascaret. *C.R. Acad. Sci. Paris*, **319**, 217–223.
- Tessier, B., Archer, A.W., Lanier, W.P.** and **Feldman, H.R.** (1995) Comparison of ancient tidal rhythmites (Carboniferous of Kansas and Indiana, USA) with modern analogues (the Bay of Mont-Saint-Michel, France). *Spec. Pubs. Int. Ass. Sediment.*, **24**, 259–271.
- Tessier, B., Billeaud, I.** and **Lesueur, P.** (2006) The Bay of Mont-Saint-Michel northern littoral: an illustrative case of sedimentary body evolution and stratigraphic organization in a transgressive/ highstand context. *Bulletin de la Société Géologique de France*, **177**, 71–78.
- Tessier, B., Billeaud, I.** and **Lesueur, P.** (2010) Stratigraphic organisation of a composite macrotidal wedge: the Holocene sedimentary infilling of the Mont-Saint-Michel Bay (NW France). *Bulletin de la Société Géologique de France*, **181**, 99–113.
- Tessier, B., Furgerot, L.** and **Mouazé, D.** (2017) Sedimentary signatures of tidal bores: a brief synthesis. *Geo-Mar. Lett.*, **37**, 325–331.
- Tessier, B., Weill, P., Billeaud, I., Furgerot, L., Campos-Soto, S., Mouazé, D., Caline, B.** and **Bonnot-Courtois, C.** (2021) The Bay of Mont Saint Michel. Sedimentary facies, morphodynamics and Holocene evolution of a hypertidal coastal system. *Geol. Field Trip Maps*, **14**, 1–39.
- Thulborn, T.** (1990) *Dinosaur tracks*, p. 410. Chapman and Hall, London.
- Turner, P.L., Kalkingham, P.L.** and **Gatesy, S.M.** (2020) It is in the loop: shared sub-surface foot kinematics in birds and other dinosaurs shed light on a new dimension of fossil track diversity. *Biol. Lett.*, **16**, 20200309.
- Van Loon, A.J.** (2009) Soft-sediment deformation structures in siliciclastic sediments: an overview. *Geologos*, **15**, 3–55.
- Varejao, F.G., Warren, L.V., Simoes, M.G., Cerri, R.I., Alessandretti, L., Santos, M.G.M.** and **Assine, M.L.** (2022) Evaluation of distinct soft-sediment deformation triggers in mixed carbonate-siliciclastic systems: Lessons from the Brazilian Pre-Salt analogue Crato Formation (Araripe Basin, NE Brazil). *Marine Petrol. Geol.*, **140**, 105673.

Manuscript received 27 July 2023; revision accepted 10 July 2024

Supporting Information

Additional information may be found in the online version of this article:

Video S1. Video showing the processes occurring during the formation of human tracks in some semi-liquid sediments located in the upper intertidal flats at Pointe du Grouin du Sud (see location in Figs 1D and 2A).

Video S2. Video showing the formation and infilling of track shown in Fig. 8A and D.

Video S3. Video showing the formation and infilling of track shown in Fig. 8B and E.